AD-A174 954 OPTIMAL AND INSENSITIVE CONTROL OF HYPERBOLIC DISTRIBUTED PARAMETER SYSTE..(U) WISCONSIN UNIV-MADISON DEPT OF MATHEMATICS D L RUSSELL JAN 86 1/1

UNCLASSIFIED AFOSR-TR-86-2107 AFOSR-84-0088 F/G 20/11 NL

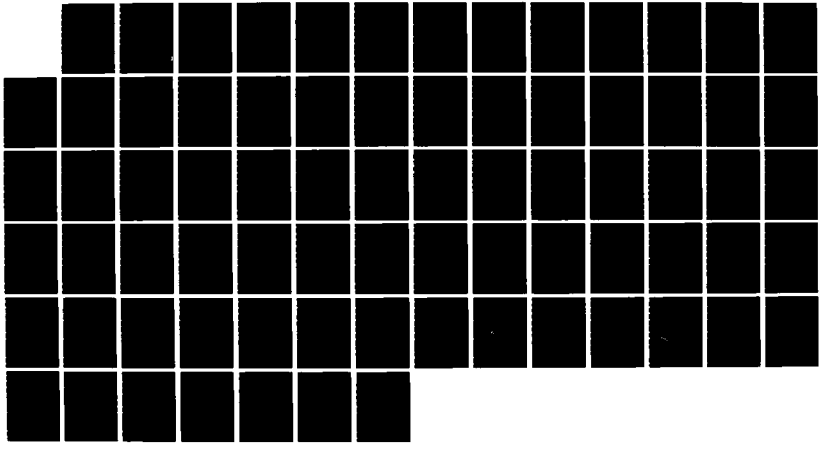

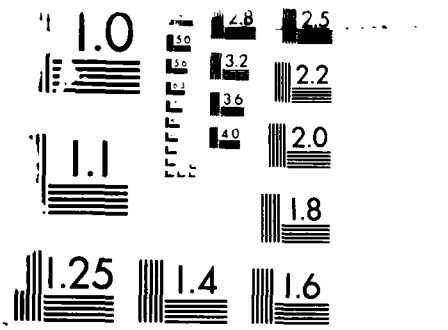
1.0
1.1
1.25
1.4
1.6
1.8
2.0
2.2
2.5
2.8
3.2
3.6
4.0

AD-A174 954

REPORT DOCUMENTATION PAGE

1b. RESTRICTIVE MARKINGS	
2a. SECURITY CLASSIFICATION AUTHORITY UNCLASSIFIED	3. DISTRIBUTION / AVAILABILITY OF REPORT Approved for public release; distribution unlimited
2b. DECLASSIFICATION / DOWNGRADING SCHEDULE	
4. PERFORMING ORGANIZATION REPORT NUMBER(S)	5. MONITORING ORGANIZATION REPORT NUMBER(S) AFOSR-TR- 86-2187
6a. NAME OF PERFORMING ORGANIZATION University of Wisconsin 6b. OFFICE SYMBOL (If applicable)	7a. NAME OF MONITORING ORGANIZATION Air Force Office of Scientific Research
6c. ADDRESS (City, State, and ZIP Code) Department of Mathematics Madison, Wisconsin	7b. ADDRESS (City, State, and ZIP Code) Directorate of Mathematical & Information Sciences, Bolling AFB DC 20332-6448
8a. NAME OF FUNDING / SPONSORING ORGANIZATION AFOSR 8b. OFFICE SYMBOL (If applicable) NM	9. PROCUREMENT INSTRUMENT IDENTIFICATION NUMBER AFOSR 84-0088
8c. ADDRESS (City, State, and ZIP Code) BP 410 Bolling AFB DC 20332-6448	10. SOURCE OF FUNDING NUMBERS PROGRAM ELEMENT NO. / PROJECT NO. 2304 / TASK NO. A5 / WORK UNIT ACCESSION NO.

11. TITLE (Include Security Classification) OPTIMAL AND INSENSITIVE CONTROL OF HYPERBOLIC DISTRIBUTED PARAMETER SYSTEMS WITH APPLICATIONS TO WING FLUTTER PROBLEMS

12. PERSONAL AUTHOR(S) David L. Russell

13a. TYPE OF REPORT	13b. TIME COVERED	14. DATE OF REPORT (Year, Month, Day)	15. PAGE COUNT
FINAL	FROM 2/84 TO 1/86		

16. SUPPLEMENTARY NOTATION

17. COSATI CODES			18. SUBJECT TERMS (Continue on reverse if necessary and identify by block number)
FIELD	GROUP	SUB-GROUP	

19. ABSTRACT (Continue on reverse if necessary and identify by block number)

During the period covered by the grant the PI wrote 5 papers. The titles include: "On the Dirichlet / Neumann Boundary Control Problem Associated with Maxwell's Equations in a Cylindrical Region"; "A Floquet decomposition for Volterra Equations with Periodic Kernel and a transform Approach to Linear Recursion Equations"; and "Mathematical Models for the Elastic Beam and their Control-Theoretic Implications";

20. DISTRIBUTION / AVAILABILITY OF ABSTRACT	21. ABSTRACT SECURITY CLASSIFICATION
☐ UNCLASSIFIED/UNLIMITED ☒ SAME AS RPT. ☐ DTIC USERS	

22a. NAME OF RESPONSIBLE INDIVIDUAL	22b. TELEPHONE (Include Area Code)	22c. OFFICE SYMBOL
Brian Woodruff, MAJOR, USAF	202/676-5207	NM

DD FORM 1473, 84 MAR 83 APR edition may be used until exhausted. All other editions are obsolete.

SECURITY CLASSIFICATION OF THIS PAGE

FINAL SCIENTIFIC REPORT ON

AFOSR GRANT 84 - 0088

David L. Russell, Principal Investigator

Department of Mathematics

University of Wisconsin - Madison

Madison, WI 53706

1. General. The subject grant supported research work in control of distributed parameter systems, control of nonlinear systems, and the mathematical modelling of such systems by the Principal Investigator and his research assistants during the period Feb. 15, 1984 - Oct. 15, 1985. In addition to salary support for the Principal Investigator and his research assistants, funds were used to bring visitors to the University of Wisconsin campus as scientific consultants for short periods, to support scientific computing relevant to the research program, to support domestic and foreign travel by the Principal Investigator and to purchase needed equipment and supplies for the UW MIPAC (Modelling, Information Processing and Control) Facility, for which the Principal Investigator serves as coordinator. Below we describe these activities in greater detail. A copy of a recent research article is attached as an Appendix to this report.

2. Areas of Research Emphasis. During the grant period a wide ranging program of scientific research in mathematical systems theory was carried forward. In the rest of this section we summarize progress in:

(a) Control Theory of Distributed Parameter Systems;

(b) Control of Nonlinear Systems;

(c) Modelling of Distributed Parameter Systems;

(d) Coefficient Identification in Distributed Systems.

(a) The Principal Investigator has worked and supervised research in the area of control of distributed parameter systems for many years, developing theories applicable to wave (hyperbolic) processes and diffusion (parabolic) processes as well as many other areas important in applications. During the grant period two research assistants were supervised in carrying out doctoral dissertation work in these areas.

The first of these assistants, Richard Rebarber, received the PhD. degree in August, 1984. His dissertation was concerned with control canonical forms and spectral assignment problems related to control of infinite dimensional systems generically described by

$$\dot{x} = A\,x + B\,u$$

wherein the operator A is the generator of a holomorphic semigroup. Because of recent experimental evidence and related mathematical modelling work, which we describe under (iii) below, it is now clear that the most realistic models for vibration of beams, plates, etc., are actually systems of this sort, involving frequency-proportional damping. Rebarber's results deal with the extent to which the closed loop spectrum of the system obtained with linear feedback $u = K\,x$ can be specified by choice of the feedback operator A.

A second assistant, Katherine Kime, is expected to receive the PhD. degree in August, 1986. During the grant period she was partially supported with grant funds in her research on control of electromagnetic fields, satisfying the Maxwell equations, by means of electric currents flowing on the boundary of the spatial region in which the fields are defined. This research has extended earlier work carried out by the Principal Investigator under AFOSR auspices. Ms. Kime has been able to demonstrate the controllability of finite energy states in a three dimensional spherical region and, with additional smoothness requirements, in more general regions. We expect the work ultimately to have implications for design of radar non-reflecting surfaces, etc.

(b) We have been interested for some time in the control of nonlinear systems exhibiting self-excited oscillations because of their importance in the study of flutter phenomena in aircraft design. Emphasis has been placed on systems of the form

$$\dot{x} = A\,x + B\,u + C\,y$$

$$\dot{y} = g(x,u,y)$$

wherein x is the state of an elastic system with basically linear dynamics and y is the state of a (generally lower dimensional) nonlinear system interracting with the elastic system to produce nonlinear oscillations whose amplitudes may become large as their frequency approaches one of the resonant frequencies of the elastic structure. We are concerned not only with the question of using the control input, u, to alleviate the effects of the self-excited oscillations in the presence of complete information about the total system state (x,y), but also with the question of system state estimation and resultant control specification when a lower dimensional output

$$\omega = d(x,y)$$

is all that is available. A doctoral candidate, Thomas Svobodny, was supported during the grant period in the initial stages of his work in connection with this latter question. He has been seeking to extend to nonlinear systems exhibiting self-excited oscillations some work done earlier by the principal investigator concerning

adaptive rejection of periodic disturbances, v(t), in a system

$$\dot{x} = A\,x + B\,u + v$$

Promising initial results on observability of linear systems with time-periodic coefficients are being extended to be applicable to the nonlinear systems of interest. We have also been acquiring laboratory data on actual oscillating systems to serve as test cases for the identification, estimationand control procedures being developed in these researches.

(iii) During the contract period our main mathematical modelling research activity has been in the area of development of mathematical models to replicate the observed frequency-proportional "structural" damping properties of actual beams. While this work has been completed under a successor grant, AFOSR 85 - 0283, we can state unequivocally that the major conceptual advances were made under the aegis of the subject grant, AFOSR 84 - 0088, during the period when the Principal Investigator was visiting the University of Florida at Gainesville. Following many unsuccessful attempts, a model in the form of an integro-partial differential equation

$$\rho\frac{\partial^2 w}{\partial t^2} + 2\gamma\int_0^L h(x,\xi)\left[\frac{\partial^2 w}{\partial t\partial x}(x,t) - \frac{\partial^2 w}{\partial t\partial x}(\xi,t)\right]d\xi + EI\frac{\partial^4 w}{\partial x^4} = 0$$

was developed which, with γ and the "interraction kernel" $h(x,\xi)$ correctly chosen relative to the mass density ρ and bending modulus EI, results in very close spectral matching with experimental data taken from various types of beams excited into vibratory motion in a laboratory setting. We have high hopes that this model will find wide application in theoretical damping considerations relative to large space structures and other similar topics of current interest.

(iv) We have also been interested in the problem of identifying the coefficients of a partial differential equation, assumed to lie in a particular class of such equations, from data taken from solutions of the equation. Such problems arise in porous flow problems, where the potential function φ can be measured in the field and is assumed to satisfy an elliptic equation of the form

$$\nabla\cdot(p\nabla\varphi) = f$$

with p the permeability of the flow medium and f the source distribution function. A variety of L^1 and L^∞ methods admitting approximate realization in linear programming codes have been studied and tested computationally with very promising results. A graduate research assistant, Robert Acar, has been working with the Principal Investigator in this area.

A second type of identification problem concerns equations of evolution type describing vibrations of physical continua, such as the wave equation

$$r\frac{\partial^2 w}{\partial t^2} - \frac{\partial}{\partial x}\left[k\frac{\partial w}{\partial x} \right] = 0$$

or the beam equation (undamped here)

$$\rho\frac{\partial^2 w}{\partial t^2} + \frac{\partial^2}{\partial x^2}\left[EI\frac{\partial^2 w}{\partial x^2} \right] = 0 \ .$$

It is assumed that a scalar functional of the state is recorded, whose power spectrum reveals the natural frequencies of vibration of the system. The problem is to recover whatever information is recoverable about the coefficient functions of the system from the spectral data at hand. A perturbation procedure based on spanning and independence properties of the squared eigenfunctions has been initially formulated and will be a subject for future study.

3. Other Scientific Activities under AFOSR 84 - 0088.

(a) Visitors. Grant funds were used to bring a number of visitors to the U.W. campus for short-term scientific consulting purposes. These visitors, with the approximate duration of their stay, their home affiliation and their area of expertise, included:

E. Fernandez (3 weeks) VPI, Functional Equations;
K. Kunisch (3 days) Univ. of Graz, Identification;
Q. Iqbal (3 weeks) Univ. of Karachi, Algebraic Systems.

(b) Travel. Grant funds were used to support domestic travel by the Principal Investigator to the 1984 Control and Decision Conference in San Antonio, Texas and to AFOSR headquarters in the spring of 1985. Funds also supported attendance by the Principal Investigator and his assistant, Robert Acar, at the October, 1985 meeting on Systems Identification and related topics at the University of Oklahoma in Norman, OK. Foreign travel sponsored by the grant consisted of the July, 1984 trip to Vorau and Graz, Austria, for the 1984 Vorau Conference on Identification and Control of Distributed Parameter Systems and for a week of scientific meetings in Graz with Professors Kappel and Kunisch.

(c) Scientific Computing, Supplies, Equipment. Grant funds were used to purchase time for scientific computing on the UW MACC Univac 1110 Computer for use by the Principal Investigator and his assistants. Funds were also used for various categories of supplies and office needs such as stationery, postage, long distance telephone calls, etc. A variety of equipment to be used in the construction of laboratory models for study and comparison with mathematical models was purchased and put into use in the UW MIPAC Model Development Unit at 1307 University Ave., Madison. Certain modifications to MIPAC's HP5451C Fourier Analyzer were paid for with grant funds and a variety of related supplies such as computer discs and tapes, graphics supplies, model construction supplies, etc. were paid for with grant funds. Details will be provided in the Financial Report prepared by our Office of Research Administration, Financial.

4. Publications Issued During the Grant Period.

Grant funds sponsored research resulting in a number of scientific reports issued over the lifetime of the grant and paid for their preparation and, in some cases, for journal reprints. A list of these publications follows:

1. On the Dirichlet-Neumann boundary control problem associated with Maxwell's equations in a cylindrical region. To appear in SIAM Journal on Control and Optimization, 1986.

2. Frequency/period estimation and adaptive rejection of periodic disturbances. To appear in SIAM Journal on Control and Optimization, 1986.

3. A Floquet decomposition for Volterra equations with periodic kernel and a transform approach to linear recursion equations. Submitted to the Journal of Differential Equations.

4. Mathematical models for the elastic beam and their control-theoretic implications. Proc. 1984 Autumn College on Semigroups and their Applications, Int'l. Centre for Theoretical Physics, Trieste, Italy, November 1984. To be published by Birkhauser.

The above are by the Principal Investigator. Also sponsored by the grant was the following, by Richard Rebarber:

5. Control canonical forms and spectral assignment for holomorphic semigroups. Thesis, University of Wisconsin, Madison, Aug. 1984.

APPENDIX:

"Mathematical Models for the Elastic Beam

with Frequency-Proportional Damping"

by

David L. Russell

University of Wisconsin, Madison

ON MATHEMATICAL MODELS FOR THE ELASTIC BEAM WITH FREQUENCY-PROPORTIONAL DAMPING*

by

David L. Russell†

Coordinator, UW MIPAC Facility

Mathematics Research Center

University of Wisconsin, Madison

* Research supported in part by the U.S. Air Force Office of Scientific Research under Grants 84 - 0088 and 85 - 0283

† Department of Mathematics, University of Wisconsin, Madison

Madison, WI 53706

1. Introduction to Elementary Theories of Elastic Beam Motion

The less-than-dashing, rather pedestrian term "beam" has a guaranteed soporific effect on all but the more dedicated devotees of the science of structural mechanics. But it refers, of course, to the indispensable linear structural elements (those seeking new terminology, please take note!) without which many complex constructions would be infeasible. Consequently, it is not surprizing that mathematical models for the elastic beam have an ancient and honorable pedigree attested to by the attentions of some of the most honored historical and current figures of applied mathematics.

The Euler - Bernoulli equation for the motion of thin elastic beams is at least two hundred years old. Denoting the mass density, per unit length, by $\rho(x)$ and the second moment of the modulus of elasticity about the elastic axis (about which the first moment of the modulus of elasticity vanishes) by $EI(x)$, $0 \leq x \leq L$, it is assumed that the energy associated with motion in the x,w plane, in which the elastic axis is given by $w = 0$, can be adequately represented by

$$\mathcal{E}\left(w, \frac{\partial w}{\partial t}\right) = \int_0^L \left[\rho \left(\frac{\partial w}{\partial t} \right)^2 + EI \left(\frac{\partial^2 w}{\partial x^2} \right)^2 \right] dx \ . \qquad (1.1)$$

If it is assumed that no work is done on the beam, either by externally applied forces or by internal dissipative mechanisms, an easy application of the principle of virtual work shows that the motion must be governed by the partial differential equation

$$\rho \frac{\partial^2 w}{\partial t^2} + \frac{\partial^2}{\partial x^2} \left(EI \frac{\partial^2 w}{\partial x^2} \right) = 0 \qquad (1.2)$$

together with "natural boundary conditions" (four are required in all) implying that

$$EI \frac{\partial^2 w}{\partial x^2} \frac{\partial^2 w}{\partial t \partial x} \Bigg|_0^L - \frac{\partial}{\partial x} \left(EI \frac{\partial^2 w}{\partial x^2} \right) \Bigg|_0^L = 0 \ .$$

A variety of conditions, corresponding to different kinematic and dynamic assumptions, suffice for this purpose. The "cantilever"

configuration, wherein the beam is clamped at one end, say $x = 0$, and left free at the other, $x = L$, is described by

$$w(0,t) = 0, \quad \frac{\partial w}{\partial x}(0,t) = 0, \tag{1.3}$$

$$EI(L)\ \frac{\partial^2 w}{\partial x^2}\ (L,t) = 0, \quad -\frac{\partial}{\partial x}\ (EI\ \frac{\partial^2 w}{\partial x^2})\Big|_{x\ =\ L} = 0\ . \tag{1.4}$$

If a lateral force, φ, and moment, μ, act at $x = L$, then the right hand sides of the equations in (1.4) are replaced by μ and φ, respectively. We will describe some other cases subsequently.

The Rayleigh beam model is a fairly modest modification of the Euler - Bernoulli model, dating back some hundred years or so. To obtain it the beam element of width δ centered at x is additionally endowed with mass moment of inertia $\delta\ I_\rho(x)$. The term $I_\rho \left[\frac{\partial^2 w}{\partial t \partial x} \right]^2$ is added to the energy integrand of (1.1) and there results the partial differential equation

$$\rho\ \frac{\partial^2 w}{\partial t^2} - \frac{\partial}{\partial x}\left[I_\rho\ \frac{\partial^3 w}{\partial t^2 \partial x} \right] + \frac{\partial^2}{\partial x^2}\left[EI\ \frac{\partial^2 w}{\partial x^2} \right] = 0 \tag{1.5}$$

with corresponding modifications of the boundary conditions which we will not detail at this point.

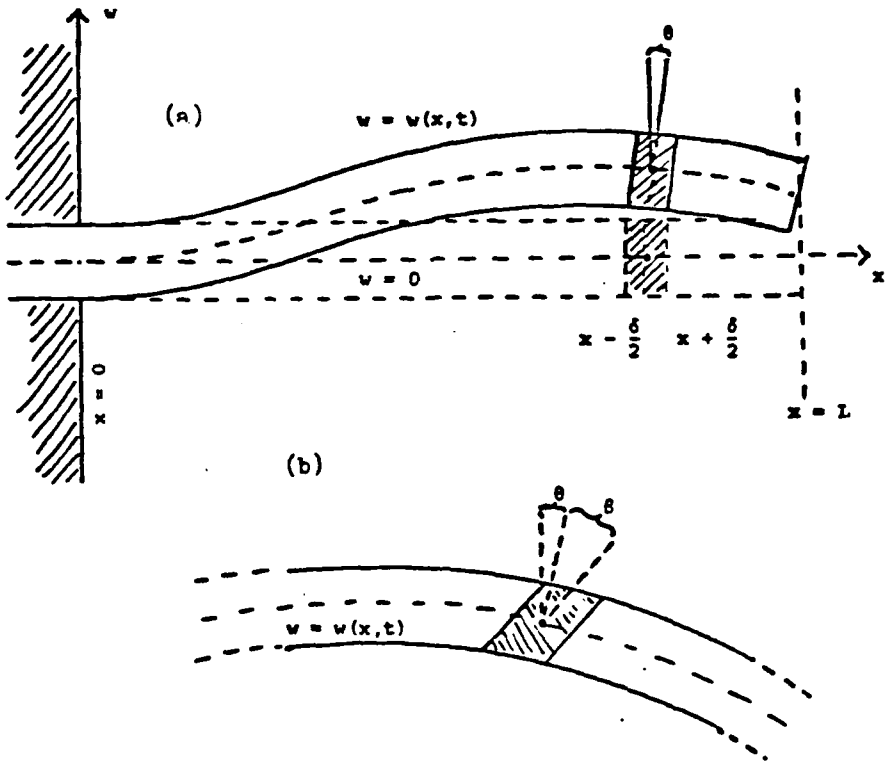

Fig. 1.1

The Timoshenko beam model goes back about fifty years and represents a more radical departure from the simple Euler-Bernoulli theory than does the Rayleigh model. In the Timoshenko model [7] beam elements undergo not only rigid motions, as is assumed in the previous two models, but also undergo a shearing motion so that an originally rectangular w,x cross section is transformed into a parallellogram as shown in Figure 1(b). The total rotation angle of an element is thus

$$\Psi(x,t) = \theta(x,t) + \beta(x,t)$$

where for small motions the bending angle θ is given approximately by

$$\theta(x,t) \simeq \frac{\partial w}{\partial x}(x,t)$$

and β is the angle of shear. Consequently

$$\beta(x,t) \simeq \Psi(x,t) - \frac{\partial w}{\partial x}(x,t) \ .$$

The energy expression used is

$$\mathcal{E}(w,\frac{\partial w}{\partial t},\psi,\frac{\partial \psi}{\partial t}) = \int_0^L \left[\rho\left(\frac{\partial w}{\partial t} \right)^2 + I_\rho\left(\frac{\partial \psi}{\partial t} \right)^2 + K\left(\psi - \frac{\partial w}{\partial x} \right)^2 + EI\left(\frac{\partial \psi}{\partial x} \right)^2 \right] dx,$$

where $K(x)$ is the modulus of elasticity in shear. Again, application of the principle of virtual work quickly leads to the Timoshenko equations

$$\rho \frac{\partial^2 w}{\partial t^2} - \frac{\partial}{\partial x}\left(K \frac{\partial w}{\partial x} - \psi \right) = 0 , \tag{1.6}$$

$$I_\rho \frac{\partial^2 \psi}{\partial t^2} - \frac{\partial}{\partial x}\left(EI \frac{\partial \psi}{\partial x} \right) + K\left(\psi - \frac{\partial w}{\partial x} \right) = 0 . \tag{1.7}$$

As inspection quickly shows, these equations have the form of two coupled wave equations. In general the wave speeds $\left[K(x)/\rho(x)\right]^{1/2}$ and $\left[EI(x)/I_\rho(x)\right]^{1/2}$ are different, resulting in a hyperbolic system with four families of characteristic curves, consisting of two pairs, each pair corresponding two waves of the same speed moving in opposite directions. The boundary conditions come out of the same calculations as produce the equations (1.6) and (1.7). In the case of the cantilever configuration these conditions are easily seen to take the form

$$w(0,t) = 0, \ \psi(0,t) = 0, \tag{1.8}$$

$$K(L)\left[\frac{\partial w}{\partial x}(L,t) - \psi(L,t) \right] = \varphi(t), \quad EI(L)\frac{\partial \psi}{\partial x}(L,t) = \mu(t), \tag{1.9}$$

where, again, φ and μ are the applied lateral force and moment respectively, at $x = L$.

In the constant coefficient case, if I_ρ and EI are small in comparison with K, as tends to be the case for thin beams, the first equation can be differentiated with respect to x, solved for $\frac{\partial^2 \psi}{\partial x^2}$ and substituted into the second equation to obtain

$$\rho\frac{\partial^2 w}{\partial t^2} - I_\rho \frac{\partial^4 w}{\partial t^2 \partial x^2} + EI \frac{\partial^4 w}{\partial x^4} + \frac{\rho}{K}\left[I_\rho \frac{\partial^4 w}{\partial t^4} - EI \frac{\partial^4 w}{\partial t^2 \partial x^2} \right] = 0 ,$$

which is seen to be a singular perturbation of the Rayleigh equation with ρ/K as the small parameter. Similar, but more complex, results can be obtained in the variable coefficient case and the boundary conditions may be re-expressed in terms of w also.

A model related to that of Timoshenko, but more comprehensive, has recently been developed by Antman [A], and there are many others. ~~All of the relatively simple models are traditionally compared with the "exact" three dimensional theory of Pochhammer and Chree [B], [C] for accuracy in predicting natural frequencies, modal forms, etc.~~ In this regard, from our point of view, it is preferable to let the beams "speak for themselves". Figure 1.2 shows the logarithmic power spectrum for excited vibrations of a thin steel beam, measured in the UW MIPAC laboratory. The peaks evident in the graph correspond to the natural frequencies of vibration. In this case they conform quite nicely to those predicted from the Euler - Bernoulli theory with very slight corrections from the Rayleigh model proving helpful in the higher ranges.

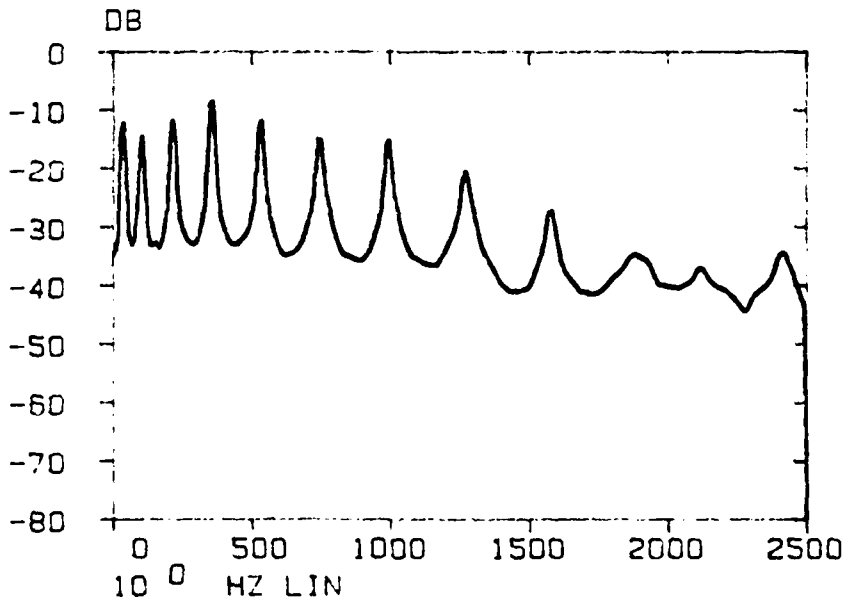

Fig. 1.2

2. Internal Damping Mechanisms.

In traditional applications it is possible to ignore internal damping effects to a large degree. This is the case because, in those applications interest is largely confined to static deformation or, at a slightly more sophisticated level, to the vibrations produced by periodically imposed loads, such as might be produced, for example, by a train of heavy cars crossing a bridge or a powerful rotating engine mounted on an aircraft wing. Damping effects in these cases can be largely ignored because the standard rule of design is to keep the natural frequencies of vibration of the structure well separated from the frequencies of expected periodic loads.

As aircraft have grown ever more sophisticated and, particularly, as the construction of platforms in space has been contemplated, it has become increasingly necessary to take internal energy losses into account. As structures have grown lighter and stronger they have also become more elastic and hence more subject to vibration problems. At the same time, pointing accuracy and platform stability requirements have made the suppression of such vibrations absolutely essential. It has become necessary to augment natural damping by the introduction of active control mechanisms and/or carefully matched passive damping systems. Paradoxically, as more elastic structures with less inherent damping have evolved, and as active control has increasingly been brought to bear, the importance of a thorough understanding of natural damping mechanisms and of a capability to accurately estimate its effects has become more, rather than less, essential. This is true because artificial damping achieved through active control implementation is inevitably limited in band width; at higher frequencies its effectiveness decreases or disappears entirely - indeed, phase lags may result in positive, rather than negative, work being done by the control forces on the higher frequency modes. That the controls used are generally effective is largely thanks to the fact that natural damping mechanisms tend to become stronger with increasing frequency, so that artificial controls can concentrate on suppression of the modes associated with lower frequencies, leaving higher frequency "spillover" effects to be "mopped up" by the strong internal damping operative at the higher end of the spectrum. As internal damping decreases, it is ever more important to be able to estimate its precise strength so that the band width requirements for the applied

active controls can be appropriately specified.

That damping rates tend to increase with frequency has long been understood. Thus simplistic models for damping such as

[P,Q,R]

$$\rho \frac{\partial^2 w}{\partial t^2} + 2\gamma \frac{\partial w}{\partial t} + \frac{\partial^2}{\partial x^2}\left[EI \frac{\partial^2 w}{\partial x^2} \right] = 0 ,$$

which produce uniform damping rates, ~~cannot be taken seriously~~ are generally not adequate. The recognition that damping rates in beams increase with increasing frequency goes back at least to Lord Kelvin in Britain and Robert Voigt, a distinguished German physicist, both working at the end of the last century [N]. The Kelvin - Voigt damping model applies, in principle, to the vibrations of any linear elastic system. The model hypothesizes that, whatever the linear operator describing the elastic restoring forces may be, the damping forces involve a positive multiple of that operator acting on the system velocity rather than the displacement. This theory, modifying the basic Euler - Bernoulli model, yields an equation which may be taken to have the form

$$\rho \frac{\partial^2 w}{\partial t^2} + 2\gamma\rho \frac{\partial^3}{\partial t \partial x^2}\left[EI \frac{\partial^2 w}{\partial x^2} \right] + \frac{\partial^2}{\partial x^2}\left[EI \frac{\partial^2 w}{\partial x^2} \right] = 0$$

with appropriately modified boundary conditions. If the fourth order elasticity operator is denoted by

$$Aw = \frac{1}{\rho} \frac{\partial^2}{\partial x^2}\left[EI \frac{\partial^2 w}{\partial x^2} \right]$$

then the operational form of the equation is

$$\frac{d^2 w}{dt^2} + 2\gamma A \frac{dw}{dt} + Aw = 0 . \qquad (2.1)$$

If the eigenvalues of the positive self-adjoint operator A are λ_k, so that the natural frequencies of the undamped system are $\omega_k = (\lambda_k)^{1/2}$, then the damped system (2.1) may be seen to have exponential solutions $e^{\sigma_k t}\varphi_k$, where φ_k is the corresponding eigenvector of

A and σ_k satisifes the quadratic equation

$$\sigma_k^2 + 2\gamma\omega_k^2\sigma_k + \omega_k^2 = 0 \ .$$

Thus σ_k is given by

$$\sigma_k = -\gamma\omega_k^2 \pm \left\{ \gamma^2\omega_k^4 - \omega_k^2 \right\}^{1/2} \ . \qquad (2.2)$$

Assuming γ to be small, we see that the σ_k are complex for some finite number of values of k with the damping rate proportional to the square of the frequency. Critical damping occurs for $\omega = 1/\gamma$; for ω_k larger than this the modes are overdamped with one of the values given by (2.2) going to $-\infty$ and the other tending to the value $\frac{-1}{2\gamma}$. The values σ_k , in fact, lie in the locus shown in Figure 2.1, consisting of a circle of radius $\frac{1}{2\gamma}$, centered at the point $(\frac{-1}{2\gamma},0)$ and the portion of the negative real axis to the left of $(\frac{-1}{\gamma},0)$. For very small values of γ all we would expect to see would be the quadratic dependence of the damping rate on the frequency. Whether the overdamping predicted by the model has ever been observed in the laboratory is unknown to this writer but it seems, on the face of it, to be unlikely.

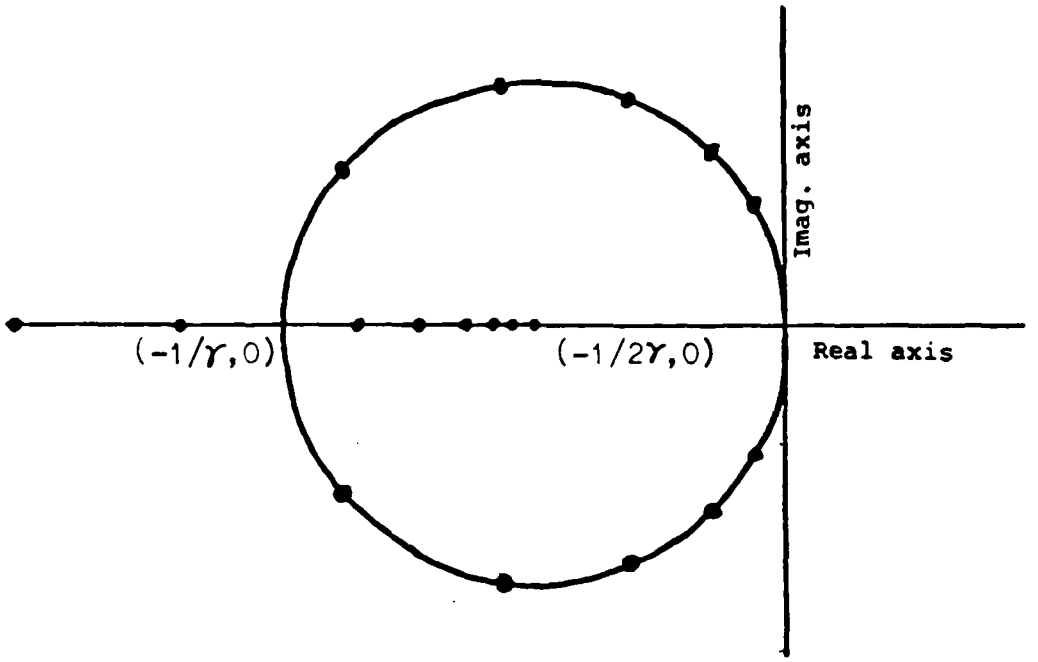

Fig. 2.1

In any case, as we will document in the final section of this paper, our experiments at UW MIPAC, in agreement with experimental data acquired by many other researchers, indicates a predominantly linear relationship between the damping rate and the frequency; a behavior widely known as structural damping. [5] We will also see, both from the experimental and theoretical point of view, that damping of this sort is by no means a "rule of nature"; indeed there is some reasons to believe that it may only apply to thin beams for which the Euler - Bernoulli model is adequate in the conservative case. More on this later.

There is no difficulty in obtaining mathematical models which exhibit this sort of damping/frequency relationship. Representing an arbitrary linear oscillator, without damping, by

$$\frac{d^2w}{dt^2} + Aw = 0 \ ,$$

the simplest mathematically viable example of a system exhibiting structural damping behavior, treated extensively by the author and G. Chen in [E], is given by

$$\frac{d^2w}{dt^2} + 2\gamma\, A^{1/2}w + Aw = 0 \ , \tag{2.3}$$

where $A^{1/2}$ denotes the positive square root of the positive self-adjoint operator A and $\gamma > 0$. Attempting a solution of the form $e^{\sigma_k t}\varphi_k$ again, we find now that

$$\sigma_k = (-\gamma \pm (\gamma^2 - 1)^{1/2})\ \omega_k$$

so that, for $0 < \gamma < 1$ the σ_k lie on the rays in the left half plane, shown in Figure 2.2, making an angle

$$\alpha = \tan^{-1}\left[\gamma/(1 - \gamma^2)\right]$$

with the imaginary axis.

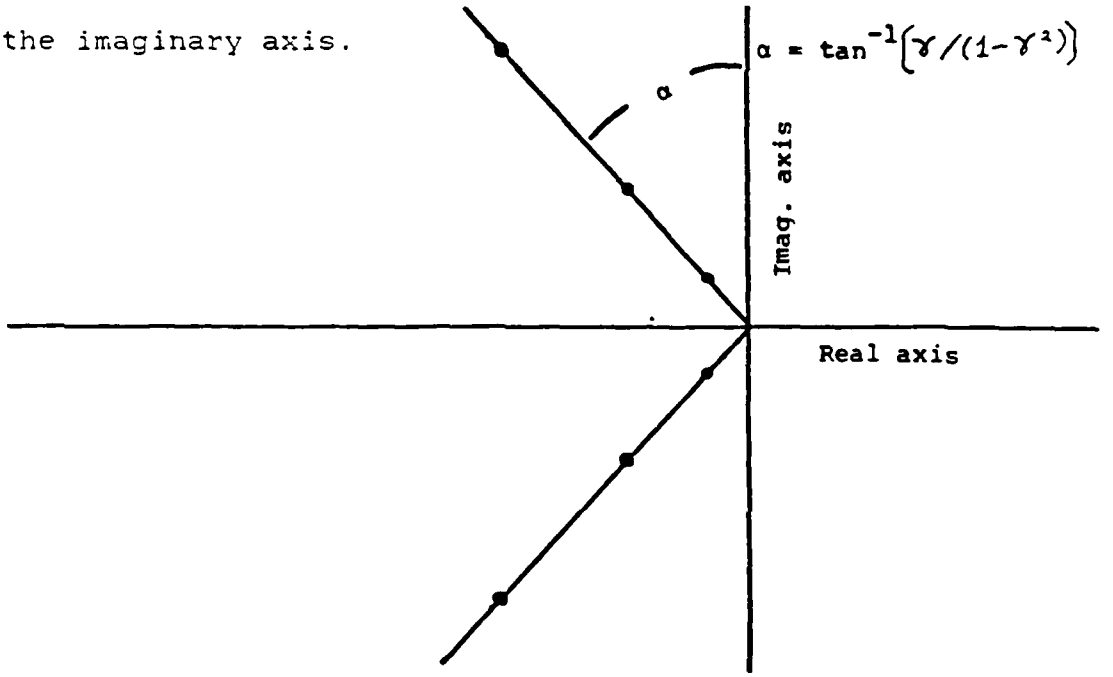

Fig. 2.2

To explain why we cannot embrace the model (2.3) with unrestrained enthusiasm, let us consider the constant coefficient case wherein

$$Aw = \frac{EI}{\rho} \frac{\partial^4 w}{\partial x^4} \quad . \tag{2.4}$$

Let us denote boundary conditions for this operator generically by

$$< \ell \ , \ w > = 0, \tag{2.5}$$

where ℓ is a linear functional defined on the domain of A. We will say that the boundary conditions given for A are <u>paired</u> if for each boundary condition (2.5) appearing in the set, the condition

$$< \ell \ , \ w'' > = 0 \tag{2.6}$$

appears in the set also. Examples include hinged endpoints, for which (taking the endpoint in question to be x = 0)

$$w(0,t) = 0, \quad EI \frac{\partial^2 w}{\partial x^2} (0,t) = 0,$$

and freely clamped endpoints for which (constant coefficient case)

$$\frac{\partial w}{\partial x} (0,t) = 0, \quad - EI \frac{\partial^3 w}{\partial x^3} (0,t) = 0 \ .$$

For paired boundary conditions the positive square root of the fourth order operator $\frac{\partial^4 w}{\partial x^4}$ is $- \frac{\partial^2 w}{\partial x^2}$ and, redefining γ slightly, the modified Euler equation in this case takes the form

$$\rho \frac{\partial^2 w}{\partial t^2} - 2\gamma \frac{\partial^3 w}{\partial t \partial x^2} + EI \frac{\partial^4 w}{\partial x^4} = 0 \ . \tag{2.7}$$

In this equation the damping term is rather easy to understand from the physical point of view - it is a lateral force acting on the beam which is negatively proportional to the bending rate.

In those cases where the boundary conditions for A are not paired, as in the case of clamped or free endpoints, respectively corresponding to

$$w(0,t) = 0, \quad \frac{\partial w}{\partial x}(0,t) = 0,$$

$$EI \frac{\partial^2 w}{\partial x^2}(0,t) = 0, \quad - EI \frac{\partial^3 w}{\partial x^3}(0,t) = 0,$$

for example, the positive square root of the fourth order operator is not the negative second order operator and the nature of the damping term in (2.3) is such as not to admit a ready physical interpretation in terms of the properties of standing waves in the beam. If the motion is conceived of in terms of travelling waves reflecting from the boundaries of the beam then, since the speed of travelling waves in the Euler-Bernoulli beam varies inversely with the square of the wave length, "square root" damping can be interpreted, regardless of the boundary conditions in force, as a statement that the damping exponent is proportional to the distance covered per unit time by a travelling wave of the particular wave length in question. However, this explanation seems rather suspect to the writer because the expression of standing waves in terms of travelling waves is a bit of a mathematical artifice here. The explanation would become quite appealing, however, if it could be demonstrated that in long thin beams the attenuation of travelling waves is specifically a function of distance travelled rather than other factors. The author is, at the present time, unaware of any research which may have been carried out in this direction.

The guiding philosophy in our modelling work is that a proposed mathematical model for a physical system must:

(i) Be well-posed from the mathematical point of view;

(ii) Replicate the physical phenomena observed;

(iii) Involve only equations all of whose terms can be assigned a direct physical meaning in terms of observable system properties or characteristics.

Where the boundary conditions on the beam are not paired, the model (2.3), at least as far as we understand it now, does not meet the third criterion stated and must, consequently, not be accepted as a viable model at the present time. The apparent necessity of discarding this model under the circumstances just described represents a

real loss because the system (2.3) has very attractive mathematical properties, as outlined in [E].

Since the middle term in (2.7) has a ready physical explanation as the rate of change of bending, it is tempting to try to use this equation whatever its disadvantages. If no modifications of the boundary conditions are made, as compared with the Euler - Bernoulli conditions, it is not true in general that the energy is monotone decreasing. Consider, for example, the cantilever case and the initial state

$$w(x,0) \equiv 0, \quad \frac{\partial w}{\partial t}(x,0) = x^2 - \frac{2}{3}x^3 + \frac{1}{6}x^4 \ .$$

(Note that $\frac{\partial w}{\partial t}$ is only required to lie in $L^2[0,L]$ for finite energy solutions, i.e., solutions in the state space $H^2[0,L] \times L^2[0,L]$ appropriate to the corresponding semigroup, and thus need not satisfy the boundary conditions imposed on w at the free endpoint x = L.)

$$\frac{d}{dt}\, \mathcal{E}(w(\cdot,t), \frac{\partial w}{\partial t}(\cdot,t))\Big|_{t=0} = 2\gamma \int_0^L \frac{\partial w}{\partial t}(x,0)\, \frac{\partial^3 w}{\partial t \partial x^2}(x,0)\, dx = 1/21$$

so that the energy is actually increasing during some interval after t = 0, rather than decreasing.

Undaunted by this, it is tempting next to see if some modification of the Euler - Bernoulli boundary conditions will result in solutions of (2.7) having monotone decreasing energy at all times. One can realize this by modifying the zero lateral force condition applying at an end point to

$$-2\gamma \frac{\partial^2 w}{\partial t \partial x} - EI \frac{\partial^3 w}{\partial x^3} = 0 \ . \qquad (2.8)$$

and one then finds, for smooth solutions, that the rate of change of energy is equal to

$$-2\gamma \int_0^L \left[\frac{\partial^2 w}{\partial t \partial x} \right]^2 dx \leq 0 \ . \qquad (2.9)$$

Unfortunately our satisfaction is short - lived, for we realize that the beam with free endpoints has purely inertial solutions

$$w(x,t) = w_0 + w_1 t + w_2 x + w_3 tx$$

for which (2.9) has the value $-2\gamma L w_3^2 < 0$ for $w_3 \neq 0$ even though no energy dissipation should take place in such motions; we have over done our attempt to introduce damping here. Nevertheless, the exercise is not quite a total loss. If we work a little harder and change (2.8) to

$$-EI \frac{\partial^3 w}{\partial x^3} + 2\gamma \frac{\partial^2 w}{\partial t \partial x} - \frac{2\gamma}{L} \left[\frac{\partial w}{\partial t}(L,t) - \frac{\partial w}{\partial t}(0,t) \right] = 0 \ , \qquad (2.10)$$

we then find, for smooth solutions, that

$$\frac{d}{dt} \mathcal{E}(w(\cdot,t), \frac{\partial w}{\partial t}(\cdot,t)) = -2\gamma \int_0^L \left[\frac{\partial^2 w}{\partial x \partial x}(x,t) \right]^2 dx + \frac{2\gamma}{L} \left[\frac{\partial w}{\partial t}(L,t) - \frac{\partial w}{\partial t}(0,t) \right]^2$$

and the energy is seen to be non-increasing for all solutions while remaining constant for the purely inertial motions. Condition (2.10) seems somewhat unnatural since it is non-local. In fact, we do not propose (2.10) as a completely serious solution to our problem, but this small success leads in a natural way to the more believable model which we proceed to discuss in the next section.

3. Form of the Mathematical Model.

As we have noted in the previous section, the commonly used Euler - Bernoulli beam equation, which will serve as the starting point for our discussion here, is based on conservation in time of the energy expression (1.1), i.e.,

$$\mathcal{E}(w,\frac{\partial w}{\partial t}) = \frac{1}{2}\int_0^L \left[\rho \left(\frac{\partial w}{\partial t} \right)^2 + EI \left(\frac{\partial^2 w}{\partial x^2} \right)^2 \right] dx,$$

wherein $w(x,t)$ is abbreviated to w, $\rho(x)$ and $EI(x)$ to ρ and EI, respectively. We will assume here that ρ and EI are uniformly positive on $0 \leq x \leq L$, that ρ is continuous, at least, and that EI is at least piecewise twice continuously differentiable on $[0,L]$.

Assuming for the moment that the function $w(x,t)$ describing the evolution of the beam displacement is smooth, an easy calculation shows that

$$\frac{d}{dt}\,\mathcal{E}(\,w(\cdot,t),\,\frac{\partial w}{\partial t}(\cdot,t)\,) = \int_0^L \left[\rho \frac{\partial w}{\partial t}\frac{\partial^2 w}{\partial t^2} + EI\,\frac{\partial^2 w}{\partial x^2}\frac{\partial^3 w}{\partial t \partial x^2} \right] dx \qquad (3.1)$$

and then, integrating the second term by parts,

$$\frac{d}{dt}\,\mathcal{E}(\,w(\cdot,t),\,\frac{\partial w}{\partial t}(\cdot,t)\,) =$$

$$= \int_0^L \left[\rho \frac{\partial w}{\partial t}\frac{\partial^2 w}{\partial t^2} - \underline{\frac{\partial}{\partial x}\left(EI \frac{\partial^2 w}{\partial x^2} \right)\frac{\partial^2 w}{\partial t \partial x}} \right] dx + EI\,\frac{\partial^2 w}{\partial x^2}\frac{\partial^2 w}{\partial t \partial x}\Big|_0^L . \qquad (3.2)$$

The presence of the angular velocity expression $\frac{\partial^2 w}{\partial t \partial x}$ in the underlined term indicates that its coefficient, $-\frac{\partial}{\partial x}\left(EI \frac{\partial^2 w}{\partial x^2} \right)$, should be interpreted as a restoring torque, arising due to spatially variable bending of the beam. Realizing that this coefficient represents a torque aids us in interpretation of th damping term which we now

introduce into the system via the definition

$$\tau_h(x,t) = 2\int_0^L h(x,\xi)\left[\frac{\partial^2 w}{\partial t\partial x}(x,t) - \frac{\partial^2 w}{\partial t\partial x}(\xi,t)\right] d\xi. \qquad (3.3)$$

We think of τ_h as a torque acting on the beam at the point x due to the differential rotation, as compared with the rotation at x, of the beam at points ξ "near" x. In many cases the support of the "interraction kernel" $h(x,\xi)$ would be restricted to a thin strip in R^2, centered on the line $x = \xi$. Application of Newton's second law dictates the symmetry condition

$$h(\xi,x) = h(x,\xi). \qquad (3.4)$$

In constant coefficient applications it is convenient to replace $h(x,\xi)$ by $\gamma h(x-\xi)$, where $\gamma > 0$ is used to parametrize the strength of the damping effect and $h(\eta)$ satisfies the normalization condition

$$\int_{-\varepsilon}^{\varepsilon} h(\eta)\, d\eta = 1 \qquad (3.5)$$

and the even-ness condition $h(\eta) = h(-\eta)$.

The source of the damping torque in differential rotation is best illustrated for the case of beams composed of composite materials, such as fiberglass, boron and graphite composites and wood. We may imagine that long fibers, whose modulus of elasticity, per unit cross - sectional area, is greater than that of the beam as a whole, pass through the beam, held in place by a matrix material of some sort. As the beam undergoes deformation of various sorts, beam elements at x and ξ may rotate at different rates, reflected by different values of $\frac{\partial^2 w}{\partial t\partial x}(x,t)$, $\frac{\partial^2 w}{\partial t\partial x}(\xi,t)$. If we think of the fibers themselves as having nearly constant length, differential rotation must result in movement of the fibers relative to the matrix, with accompanying friction against, or deformation (largely inelastic) of the matrix material. The result is a torque of the type which we have just described, since the net motion of the fibers relative to the matrix, within the individual beam elements, will be different on one side of the elastic axis from what it is on the other side

when differential rotation is taking place (see Figure 3.1).

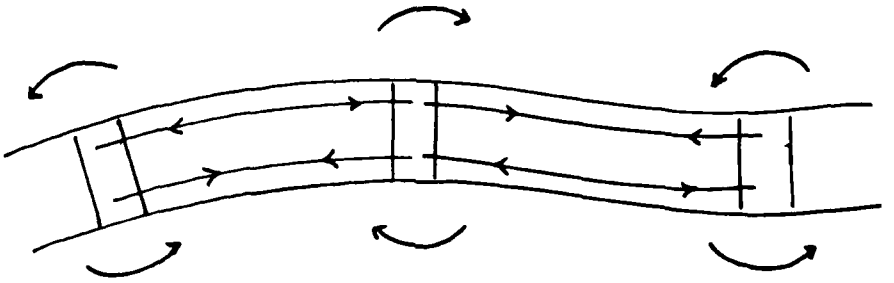

Fig. 3.1

We add the term

$$\int_0^L \tau_h(x,t)\frac{\partial^2 w}{\partial t \partial x}(x,t)\ dx$$

to both sides of (3.2), so that

$$\frac{d}{dt}\ \mathcal{E}(w(\cdot,t),\ \frac{\partial w}{\partial t}(\cdot,t)) + \int_0^L \tau_h\ \frac{\partial^2 w}{\partial t \partial x}\ dx =$$

$$\int_0^L \left\{ \rho\ \frac{\partial w}{\partial t}\ \frac{\partial^2 w}{\partial t^2} + \left[\tau_h - \frac{\partial}{\partial x}\left[EI\ \frac{\partial^2 w}{\partial x^2} \right] \right] \frac{\partial^2 w}{\partial t \partial x} \right\} dx$$

$$+ EI\ \frac{\partial^2 w}{\partial x^2}\ \frac{\partial^2 w}{\partial t \partial x}\ \Big|_0^L = \text{(with a further integration by parts)}$$

$$\int_0^L \frac{\partial w}{\partial t} \left\{ \rho\ \frac{\partial^2 w}{\partial t^2} + \frac{\partial}{\partial x}\left[\frac{\partial}{\partial x}\left[EI\ \frac{\partial^2 w}{\partial x^2} \right] - \tau_h \right] \right\} dx$$

$$+ \left\{ EI \frac{\partial^2 w}{\partial x^2} \frac{\partial^2 w}{\partial t \partial x} - \left[\frac{\partial}{\partial x} \left(EI \frac{\partial^2 w}{\partial x^2} \right) - \tau_h \right] \frac{\partial w}{\partial t} \right\} \Big|_0^L . \quad (3.6)$$

Equating the separate parts of (3.6) to zero (a procedure which can be justified by the principal of virtual work) yields the integro-partial differential equation

$$\rho \frac{\partial^2 w}{\partial t^2} + \frac{\partial}{\partial x} \left[\frac{\partial}{\partial x} \left(EI \frac{\partial^2 w}{\partial x^2} \right) - \tau_h \right] =$$

$$\rho \frac{\partial^2 w}{\partial t^2} - 2 \frac{\partial}{\partial x} \int_0^L h(x,\xi) \left[\frac{\partial^2 w}{\partial t \partial x}(x,t) - \frac{\partial^2 w}{\partial t \partial x}(\xi,t) \right] d\xi + \frac{\partial^2}{\partial x^2} \left[EI \frac{\partial^2 w}{\partial x^2} \right] = 0 \quad (3.7)$$

and the requirement that, at $x = 0$ and $x = L$,

$$EI \frac{\partial^2 w}{\partial x^2} \frac{\partial^2 w}{\partial t \partial x} - \left[\frac{\partial}{\partial x} \left(EI \frac{\partial^2 w}{\partial x^2} \right) - \tau_h \right] \frac{\partial w}{\partial t} = 0 . \quad (3.8)$$

Various beam configurations now lead to different sets of boundary conditions. For example, in the case where the beam is clamped at $x = 0$ and free at $x = L$ (i.e., the cantilever case) we obtain

$$w(0,t) = 0, \ \frac{\partial w}{\partial x}(0,t) = 0, \ \frac{\partial^2 w}{\partial x^2}(L,t) = 0, \quad (3.9)$$

$$-\frac{\partial}{\partial x} \left[EI(x) \frac{\partial^2 w}{\partial x^2} \right] \Big|_{x=L} + 2 \int_0^L h(L,\xi) \left[\frac{\partial^2 w}{\partial t \partial x}(L,t) - \frac{\partial^2 w}{\partial t \partial x}(\xi,t) \right] d\xi = 0. \quad (3.10)$$

The reader will be able to generate boundary conditions corresponding to other configurations with equal ease.

Equation (3.6) now becomes

$$\frac{d}{dt} \mathcal{E}(w(\cdot,t), \frac{\partial w}{\partial t}(\cdot,t)) = -2 \int_0^L \int_0^L h(x,\xi) \left[\frac{\partial^2 w}{\partial t \partial x}(\xi,t) - \frac{\partial^2 w}{\partial t \partial x}(x,t) \right] d\xi \frac{\partial^2 w}{\partial t \partial x}(x,t) dx$$

= (since the roles of x and ξ are symmetric and $h(x,\xi) = h(\xi,x)$)

$$= -\int_0^L \int_0^L h(\xi,x)\left[\frac{\partial^2 w}{\partial t \partial x}(x,t) - \frac{\partial^2 w}{\partial t \partial x}(\xi,t) \right] dx \, \frac{\partial^2 w}{\partial t \partial x}(\xi,t) \, d\xi$$

$$-\int_0^L \int_0^L h(x,\xi)\left[\frac{\partial^2 w}{\partial t \partial x}(\xi,t) - \frac{\partial^2 w}{\partial t \partial x}(x,t) \right] d\xi \, \frac{\partial^2 w}{\partial t \partial x}(x,t) \, dx$$

$$= -\int_0^L \int_0^L h(x,\xi)\left[\frac{\partial^2 w}{\partial t \partial x}(x,t) - \frac{\partial^2 w}{\partial t \partial x}(\xi,t) \right] \frac{\partial^2 w}{\partial t \partial x}(\xi,t) \, d\xi dx$$

$$+\int_0^L \int_0^L h(x,\xi)\left[\frac{\partial^2 w}{\partial t \partial x}(x,t) - \frac{\partial^2 w}{\partial t \partial x}(\xi,t) \right] \frac{\partial^2 w}{\partial t \partial x}(x,t) \, d\xi dx$$

$$= -\int_0^L \int_0^L h(x,\xi)\left[\frac{\partial^2 w}{\partial t \partial x}(x,t) - \frac{\partial^2 w}{\partial t \partial x}(\xi,t) \right]^2 d\xi \, dx \leq 0 . \qquad (3.11)$$

Moreover, assuming that $h(x,\xi)$ is not identically zero, the inequality is strict except in precisely the cases where $\frac{\partial^2 w}{\partial t \partial x}$ is constant, i.e., the inertial motions. Thus energy is strictly decreasing whenever the bending rate is not identically zero and is conserved when the bending rate, $\frac{\partial^3 w}{\partial t \partial x^2}$, vanishes identically.

In general the form of $h(x,\xi)$ will depend on the elasticity of the fibers of the material, as discussed earlier, the distribution of their lengths, the nature of the interface between them and the matrix material, etc. The more elastic the fibers and the shorter their average length, the more the "mass" of $h(x,\xi)$ will be concentrated near the line $\xi = x$.

For perfectly inelastic fibers, all having length L, the same length as the beam itself, $h(x,\xi)$ is a constant; call its value γ/L. Then

$$\int_0^L h(x,\xi)\ \frac{\partial^2 w}{\partial t \partial x}\ (\xi,t)d\xi = \frac{\gamma}{L}\left[\ \frac{\partial w}{\partial t}\ (L,t) - \frac{\partial w}{\partial t}\ (0,t)\ \right],$$

$$\int_0^L h(x,\xi)\ \frac{\partial^2 w}{\partial t \partial x}(x,t)\ d\xi = \gamma\ \frac{\partial^2 w}{\partial t \partial x}(x,t)\ ,$$

so that (3.7) becomes

$$\rho\ \frac{\partial^2 w}{\partial t^2} - 2\gamma\ \frac{\partial^3 w}{\partial t \partial x^2} + \frac{\partial^2}{\partial x^2}\left[\ EI\ \frac{\partial^2 w}{\partial x^2}\ \right] = 0$$

and the fourth boundary condition of the cantilever case in (3.10), for example, becomes

$$-\frac{\partial}{\partial x}\left[\ EI(x)\ \frac{\partial^2 w}{\partial x^2}\ \right]\Big|_{x\ =\ L} + 2\gamma\ \frac{\partial^2 w}{\partial t \partial x}\ (L,t) - \frac{2\gamma}{L}\ \frac{\partial w}{\partial t}\ (L,t) = 0\ ,$$

in exact agreement with the model obtained "ad hoc" at the end of the previous section.

In the case of metallic beams the "fiber" explanation used above is not persuasively valid. It may be possible to think of elongated crystal structures in the material playing much the same role as the fibers above but the analogy may well be far-fetched. The evidence for frequency-proportional damping is not quite as compelling at this writing for metallic beams as it is for composite and wooden beams, as we will see in our discussion of experimental results in Section 9.

4. Additional Properties of the Model.

Application to metallic beams, if valid at all, would necessarily involve the supposition that the fiber/crystal structures, in terms of which the damping action has been explained, are rather short. It is therefore of some interest to investigate the limiting form of the equations as the support of $h(x,\xi)$ is restricted to small neighborhoods of the line $x = \xi$.

To avoid complications with the boundary conditions here, let us consider an infinite beam, so that 0 is replaced by $-\infty$ and L by ∞. Then the energy loss term in (3.11) is

$$\int_{-\infty}^{\infty}\int_{-\infty}^{\infty} h(x,\xi)\left[\frac{\partial^2 w}{\partial t\partial x}(x,t) - \frac{\partial^2 w}{\partial t\partial x}(\xi,t)\right]^2 d\xi\, dx\ . \qquad (4.1)$$

Using the change of variables

$$y = \frac{1}{\sqrt{2}}(x+\xi),\quad \eta = \frac{1}{\sqrt{2}}(x-\xi)\ ,$$

the integral (4.1) may be rewritten as

$$\int_{-\infty}^{\infty}\int_{-\infty}^{\infty} h\left[\frac{1}{\sqrt{2}}(y+\eta),\frac{1}{\sqrt{2}}(y-\eta)\right]\left[\frac{\partial^2 w}{\partial t\partial x}\left[\frac{1}{\sqrt{2}}(y+\eta),t\right]-\frac{\partial^2 w}{\partial t\partial x}\left[\frac{1}{\sqrt{2}}(y-\eta),t\right]\right]^2 d\eta dy.$$

Now, assuming w sufficiently smooth,

$$\frac{\partial^2 w}{\partial t\partial x}\left[\frac{1}{\sqrt{2}}(y\pm\eta),t\right] = \frac{\partial^2 w}{\partial t\partial x}\left[\frac{y}{\sqrt{2}},t\right] \pm \frac{\eta}{\sqrt{2}}\int_0^1 \frac{\partial^2 w}{\partial t\partial x^2}\left[\frac{1}{\sqrt{2}}(y\pm\sigma\eta),t\right]d\sigma$$

and the integral is

$$2\int_{-\infty}^{\infty}\int_{-\infty}^{\infty} h\left[\frac{1}{\sqrt{2}}(y+\eta),\frac{1}{\sqrt{2}}(y-\eta)\right]\eta^2\left[\int_0^1 \frac{\partial^3 w}{\partial t\partial x^2}\left[\frac{1}{\sqrt{2}}(y\pm\sigma\eta),t\right]d\sigma\right]^2 d\eta dy. \qquad (4.2)$$

Consider a family of functions

$$h(x,\xi) = h_\gamma(x,\xi) \ , \ \gamma > 0 \ ,$$

each having the properties assumed earlier for $h(x,\xi)$ and such that

$$\lim_{\gamma\to 0} \int_{-\gamma}^{\gamma} h_\gamma\left(\frac{1}{\sqrt{2}}(y+\eta), \frac{1}{\sqrt{2}}(y-\eta)\right) \eta^2 \, d\eta = \frac{1}{\sqrt{2}} H\left[\frac{y}{\sqrt{2}}\right]$$

while

$$\left(\int_{-\infty}^{\gamma} + \int_{\gamma}^{\infty}\right) h_\gamma\left(\frac{1}{\sqrt{2}}(y+\eta), \frac{1}{\sqrt{2}}(y-\eta)\right) \eta^2 \, d\eta \leq J(\gamma)G(y) \ ,$$

where $H(y)$ and $G(y)$ are positive integrable functions of y and

$$\lim_{\gamma\to 0} J(\gamma) = 0.$$

Assuming that $\frac{\partial^3 w}{\partial t \partial x^2}$ is such that

$$\left[\int_0^1 \frac{\partial^3 w}{\partial t \partial x^2}\left(\frac{1}{\sqrt{2}}(y\pm\sigma\eta), t\right) d\sigma\right]^2 \leq B$$

uniformly for all y and η while

$$\left|\left[\frac{\partial^3 w}{\partial t \partial x^2}\left(\frac{y}{\sqrt{2}}, t\right)\right]^2 - \left[\int_0^1 \frac{\partial^3 w}{\partial t \partial x^2}\left(\frac{1}{\sqrt{2}}(y\pm\sigma\eta), t\right) d\sigma\right]^2\right| \leq \varepsilon(\gamma)$$

uniformly for all y in $(-\infty, \infty)$ and for η in $[-\gamma,\gamma]$, where

$$\lim_{\gamma\to 0} \varepsilon(\gamma) = 0 \ ,$$

the limiting value, as $\gamma \to 0$, of the integral (4.2) is seen to be

$$\sqrt{2}\int_{-\infty}^{\infty} H\left(\frac{1}{\sqrt{2}}\right)\left[\frac{\partial^3 w}{\partial t \partial x^2}\left(\frac{y}{\sqrt{2}}, t\right)\right]^2 dy = 2\int_{-\infty}^{\infty} H(x)\left[\frac{\partial^3 w}{\partial t \partial x^2}(x,t)\right]^2 dx. \quad (4.3)$$

Returning to equation (3.1) with 0,L replaced by $-\infty$, ∞, respectively, we see that, if the term (4.3) is added to both sides of that equation, there results

$$\frac{d}{dt}\mathcal{E}(w(\cdot,t),\frac{\partial w}{\partial t}(\cdot,t)) + 2\int_{-\infty}^{\infty} H(x)\left[\frac{\partial^3 w}{\partial t \partial x^2}(x,t)\right]^2 dx =$$

$$= \int_{-\infty}^{\infty} \left[\rho \frac{\partial w}{\partial t}\frac{\partial^2 w}{\partial t^2} + \left[2H \frac{\partial^3 w}{\partial t \partial x^2} + EI \frac{\partial^2 w}{\partial x^2} \right] \frac{\partial^3 w}{\partial t \partial x^2} \right] dx$$

= (after integrating the last product twice by parts w. resp. to x)

$$= \int_{-\infty}^{\infty} \frac{\partial}{\partial t}\left[\rho \frac{\partial^2 w}{\partial t^2} + 2\frac{\partial^2}{\partial x^2}\left[H \frac{\partial^3 w}{\partial t \partial x^2} \right] + \frac{\partial}{\partial x^2}\left[EI \frac{\partial^2 w}{\partial x^2} \right] \right] dx .$$

(Here we have, of course, assumed that w, $\frac{\partial w}{\partial t}$ and their x-derivatives tend to zero at an appropriate rate as $|x| \to \infty$.) Now the condition that the integrand should vanish identically corresponds to the Kelvin - Voigt partial differential equation

$$\rho \frac{\partial^2 w}{\partial t^2} + 2\frac{\partial^2}{\partial x^2}\left[H \frac{\partial^3 w}{\partial t \partial x^2} \right] + \frac{\partial^2}{\partial x^2}\left[EI \frac{\partial^2 w}{\partial x^2} \right] = 0 . \qquad (4.4)$$

Thus our model is consistent with the Kelvin - Voigt model, under the stated conditions, as the "mass" of $h(x,\xi)$ is progressively more concentrated near $x = \xi$. For fixed γ, equivalently fixed $h(x,\xi)$, this means that our model approximates the Kelvin - Voigt model for vibrations of large wave length, i.e., low frequency. This will be made more precise in the following material on the spectral properties of the constant coefficient equation on $(-\infty,\infty)$.

Further work of a more precise character will be required in order to obtain a rigorous argument showing that solutions of (3.7) approach solutions of (4.4) as $\gamma \to 0$ and to account for the same phenomena in finite beams with their attendant boundary conditions. We have some preliminary developments in this direction, but the work must appear elsewhere.

We pass now to a discussion of the spectral properties of the constant coefficient equation on $(-\infty,\infty)$. Taking our earlier remarks into account, the constant coefficient version of our equation, with $\eta = x - \xi$, is

$$\rho\frac{\partial^2 w}{\partial t^2} - 2\gamma\frac{\partial}{\partial x}\int_{-\infty}^{\infty} h(\eta)\left[\frac{\partial^2 w}{\partial t\partial x}(x,t) - \frac{\partial^2 w}{\partial t\partial x}(x-\eta,t)\right]d\eta + EI\frac{\partial^4 w}{\partial x^4} = 0. \qquad (4.5)$$

The function h has the properties described in (3.4), (3.5) and ρ, EI are positive constants. Equation (4.5) applies for an infinite beam or, in much the same form, for the periodic case wherein x is identified with $x + L$ for some finite $L > 0$. Our purpose in this paragraph is to study spectral properties of this equation under the assumption that $h \in L^1(-\infty,\infty)$ with $\int_{-\infty}^{\infty} h(\eta)\, d\eta = 1$. Accordingly, our equation becomes

$$\rho\frac{\partial^2 w}{\partial t^2} - 2\gamma\frac{\partial^3 w}{\partial t\partial x^2} + \int_{-\infty}^{\infty} h(\eta)\frac{\partial^3 w}{\partial t\partial x^2}(x-\eta,t)\, d\eta + EI\frac{\partial^4 w}{\partial x^4} = 0, \qquad (4.6)$$

the form which we will use for our analysis. The periodic case may be developed along quite similar lines.

We begin by looking for solutions of (4.6) in the form

$$w(x,t) = e^{\sigma t}\varphi(x)$$

leading to the steady state equation

$$\rho\sigma^2\varphi(x) - 2\gamma\sigma\varphi''(x) + \sigma\int_{-\infty}^{\infty} h(\eta)\varphi''(x-\eta)d\eta + EI\varphi^{(iv)}(x) = 0. \qquad (4.7)$$

Let

$$\Phi(\tau) = \int_{-\infty}^{\infty} e^{-i\tau x}\varphi(x)\, dx, \quad -\infty < \tau < \infty, \qquad (4.8)$$

be the Fourier transform of φ, convergent in an appropriate sense. Applying the Fourier operator to the equation we have

$$\left[\rho\sigma^2 + 2\gamma\tau^2(1 - \hat{h}(\tau))\sigma + EI\tau^4 \right] \Psi(\tau) = 0. \qquad (4.9)$$

The coefficient of $\Psi(\tau)$ must vanish on the support of the function (or distribution) $\Psi(\tau)$, leading to the following relationship between σ and τ:

$$\sigma = \sigma(\tau) = \frac{\tau^2}{\rho}\left[- g(\tau) \pm \sqrt{g(\tau)^2 - \rho EI} \right], \qquad (4.10)$$

with

$$g(\tau) = \gamma(1 - \hat{h}(\tau)). \qquad (4.11)$$

Here, as implied earlier, $\hat{h}(\tau)$ is the Fourier transform of the interraction kernel $h(\eta)$. From the integrability of $h(\eta)$ we know that $\hat{h}(\tau)$ is continuous and

$$\lim_{|\tau|\to\infty} \hat{h}(\tau) = 0. \qquad (4.12)$$

For a relatively low level of damping we may assume $\gamma^2 < \rho EI$. Then, from (4.10), (4.11), (4.12), it is clear that for large values of τ

$$\sigma \sim \frac{\tau^2}{\rho}\left[-\gamma(1-\hat{h}(\tau)) \pm i\sqrt{\rho EI-\gamma^2}\left[1 + \frac{\gamma^2\hat{h}(\tau) - \gamma^2(\hat{h}(\tau)^2/2) + \cdots}{\rho EI - \gamma^2}\right]\right]$$

$$\sim \frac{\tau^2}{\rho}\left[-\gamma \pm i\sqrt{\rho EI-\gamma^2} \right]\left[1 \mp \frac{i\gamma\hat{h}(\tau)}{\sqrt{\rho EI-\gamma^2}} \right]$$

to first order in $\hat{h}(\tau)$ as $|\tau| \to \infty$. Asymptotically, as $|\tau| \to \infty$, σ lies along the rays

$$R_{+,-} = \{ z \mid z = r(-\gamma \pm i\sqrt{\rho EI-\gamma^2}\,),\ r > 0 \}$$

in the left half complex plane.

From (3.5) it is clear that

$$\lim_{|\tau|\to 0} \hat{h}(\tau) = 1$$

so that

$$\sigma \simeq \frac{\tau^2}{\rho}\left[\ \pm i\sqrt{\rho EI-\gamma^2} + O(1)\ \right]\ ,\ |\tau| \to 0\ ,$$

showing that the spectral curve is tangent to the imaginary axis at the origin. In fact, since h is even, two integrations by parts show that

$$\hat{h}(\tau) = \int_{-\infty}^{\infty} e^{-i\tau\eta}h(\eta)d\eta = 1 - \tau^2\int_{-\infty}^{\infty} e^{-i\tau\eta}\theta(\eta)d\eta\ ,$$

where

$$\theta''(\eta) = h(\eta),\ \lim_{|\eta|\to\infty}\theta(\eta) = 0,\ \lim_{|\eta|\to\infty}\theta'(\eta) = 0.$$

Thus, as $|\tau| \to 0$,

$$\sigma \simeq \frac{\tau^2}{\rho}\left[\ -\gamma\theta\tau^2 \pm i\sqrt{\rho EI-\gamma^2}\ \right]\ ,$$

$$\theta = \int_{-\infty}^{\infty}\theta(\eta)d\eta = 1/2\int_{-\infty}^{\infty}\eta^2 h(\eta)d\eta\ .$$

Thus, at longer wave lengths, the spectrum tends to that of the corresponding Kelvin - Voigt equation, as we should expect from our earlier work in this section since taking long wave lengths for fixed h may be seen to be equivalent to allowing the support of $h(\eta)$ to contract to $\{0\}$, keeping wave length fixed. A typical spectral curve for the beam of infinite length with the proposed damping mechanism is shown in Figure 4.1.

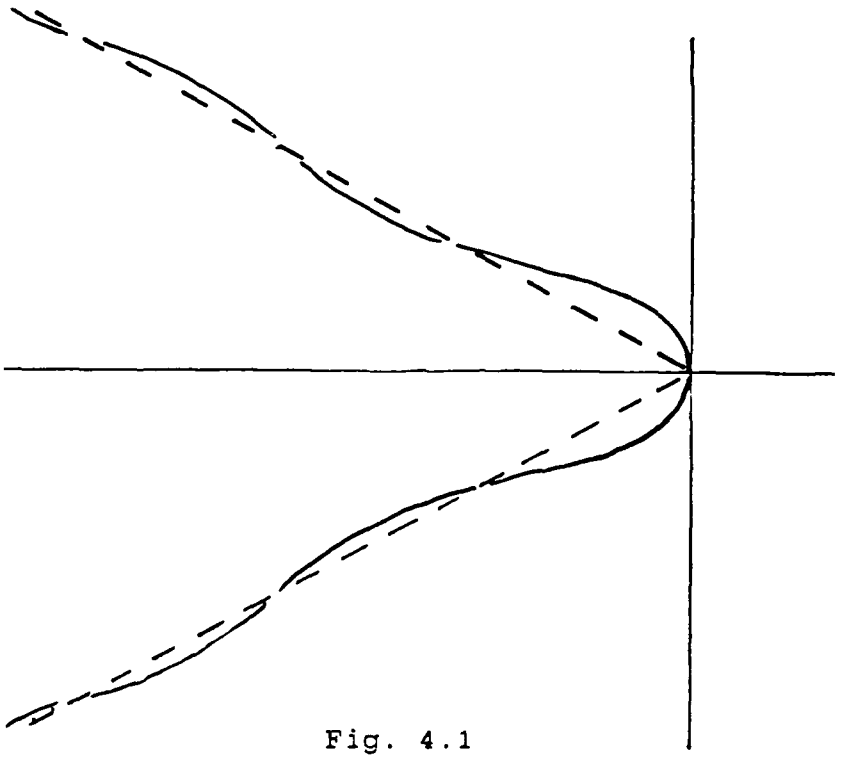

Fig. 4.1

For finite beams of large length, L, the spectrum will consist of discrete points closely spaced along a similar curve in the complex plane.

From (4.9) we have

$$\hat{h}(\tau) = 1 + \frac{EI\tau^2}{2\gamma\sigma(\tau)} + \frac{\rho\sigma(\tau)}{2\gamma\tau^2} .$$

Thus, in principle, $\hat{h}(\tau)$, and hence $h(\eta)$, can be reconstructed from the knowledge of $\sigma(\tau)$. This remains true in an approximate sense for finite beams of large length and may prove useful in identifying actual dissipation mechanisms in the laboratory.

It is interesting to note what happens when the basic, conservative, system (before damping is introduced), i.e., the Euler - Bernoulli model in the above analysis, is replaced by the Rayleigh model (1.5). The equation (4.9) is then replaced by

$$\left[(\rho + I_\rho\tau^2)\sigma^2 + 2\gamma\tau^2(1-\hat{h}(\tau))\sigma + EI\tau^4\right]\Psi(\tau) = 0$$

which leads to (cf. (4.10))

$$\sigma = \frac{\tau^2}{\rho+I_\rho\tau^2}\left[\ -g(\tau) \pm \sqrt{g(\tau)^2-(\rho+I_\rho\tau^2)EI}\ \right]$$

$$\simeq \frac{\tau^2}{\rho+I_\rho\tau^2}\left[-\gamma\pm i\sqrt{(\rho+I_\rho\tau^2)EI-\gamma^2}\ \mp \underline{\frac{i\gamma\hat{h}(\tau)}{\sqrt{(\rho+I_\rho\tau^2)EI-\gamma^2}}\left[-\gamma\pm i\sqrt{(\rho+I_\rho\tau^2)EI-\gamma^2}\right]}\right].$$

The underlined terms tend to zero as $|\tau| \to \infty$, so that

$$\mathrm{Re}(\sigma(\tau)) \to \frac{-\gamma}{I_\rho}\ ,\ |\tau| \to \infty\ ,$$

$$\mathrm{Im}(\sigma(\tau)) \to \sqrt{I_\rho EI}\ \tau\ ,\ |\tau| \to \infty\ .$$

In this case the spectral curve is initially tangent to the imaginary axis, for $|\tau|$ near zero, and tends to a line parallel to the imaginary axis, γ/I_ρ units to the left, as $|\tau| \to \infty$.

5. State Space, Boundary Conditions, Semigroup Formulation.

From the form (1.1) of the energy expression for the Euler-Bernoulli beam we are led to define the state space as a subspace, or in some cases a quotient space, of $H^2[0,L] \times L^2[0,L]$. The inner product should be consistent with the bilinear form

$$\langle (w,v),(\hat{w},\hat{v})\rangle = \int_0^L \left[\rho(x)v(x)\bar{\hat{v}}(x) + EI(x)w''(x)\overline{\hat{w}''(x)}\right]dx$$

which, in turn, is related to the energy-motivated seminorm

$$\|(w,v)\|^2 = \int_0^L \left[\rho(x)|v(x)|^2 + EI(x)|w''(x)|^2\right]dx. \qquad (5.1)$$

To do this properly it is necessary to say something about the boundary conditions, not all of which are created equal. Let B be the set of distribution pairs, in Schwartz's sense, such that the boundary conditions on the unforced beam are expressible in the form

$$\langle \beta_1, w\rangle + \langle \beta_2, v\rangle = 0 \ , \ (\beta_1,\beta_2) \in B \ . \qquad (5.2)$$

Some of these boundary conditions represent kinematic constraints while others are really dynamical equations. The former constitute a subset $C \subset D$ of pairs $(\beta,0)$, where β is a continuous linear functional on $H^2[0,L]$, which prescribe certain constraints on the beam displacement without any reference to applied forces, such as, e.g.,

$$w(0,t) = 0, \ \frac{\partial w}{\partial x}(0,t) = 0, \text{ etc.}$$

Let us denote the subspace of $H^2[0,L]$ consisting of w such that $\langle \beta, w\rangle = 0$, $(\beta,0) \in C$, by $H_C^2[0,L]$. The remaining boundary conditions, corresponding to distribution pairs in B - C, are really dynamical equations which have to do with certain forces applied to the system or, in the free case, state that certain forces are zero. Thus, in the cantilever case

$$EI\frac{\partial^2 w}{\partial x^2}(L,t) = 0, \quad -\frac{\partial}{\partial x}\left[EI\frac{\partial^2 w}{\partial x^2}\right](L,t) = 0$$

are statements that the applied torque and lateral force, respectively, at x = L, are zero. In the forced case the right hand sides would be replaced by a moment μ and a lateral force φ. Although the elements of B - C in this cantilever case still have the form $(\beta,0)$, it is clear that β is not a continuous linear functional on $H^2[0,L]$.

Let N_C be the subspace of $H_C^2[0,L] \times L^2[0,L]$ on which the semi-norm (5.1) vanishes. In many cases $N_C = \{0\}$ but not, e.g., in the case of the beam with two free endpoints, or in the case where one endpoint is free and the other hinged. Extended in the obvious way to

$$\mathcal{H} = \left[H_C^2[0,L] \times L^2[0,L] \right] / N_C$$

the semi-norm (5.1) becomes the norm for our state space, $\mathcal{H}$. We will continue to refer to state vectors as displacement and velocity pairs (w,v); the equivalence class will be understood in those cases where $N_C \neq \{0\}$.

The state space now defined, we proceed to pose our dynamical equations in that context. With z = (w,v), consider the unbounded operator on $\mathcal{H}$ defined by

$$Az = \begin{bmatrix} 0 & I \\ -A & -G \end{bmatrix} \begin{bmatrix} w \\ v \end{bmatrix},$$

where the operational definitions of A and B are

$$(Aw)(x) = (EI(x)w''(x))'', \quad (Gv)(x) = -2\frac{\partial}{\partial x}\int_0^L h(x,\xi)[v'(x)-v'(\xi)]d\xi.$$

The domain of A consists of those pairs $(w,v) \in H^4[0,L] \times H^2[0,L]$ such that (5.2) is true for all $(\beta_1,\beta_2) \in B$. Passing to equivalence classes where necessary, this is a dense subspace $\mathcal{D}(A) \subset \mathcal{H}$

and $\mathbb{A}$, so defined, is a closed operator. Our model equation (3.7) together with the boundary conditions arising from (3.8), and discussed earlier, is then equivalent to

$$\dot{z} = \mathbb{A}z \ . \tag{5.3}$$

The computation (3.11) can then be used, with a few refinements, to show that $\mathbb{A}$ is dissipative, i.e.,

$$\langle z, \mathbb{A}z \rangle \leqq 0, \ z \in \mathcal{D}(\mathbb{A}) \ .$$

From this it follows immediately (see, e.g., [F], [G]) that $\mathbb{A}$ generates a strongly continuous semigroup, $Z(t)$, of bounded operators on $\mathcal{H}$.

It turns out that the semigroup $Z(t)$ is, in fact, a holomorphic semigroup, as one might expect from the location of the spectrum in the constant coefficient, infinite length case discussed earlier. A general idea of the proof of holomorphicity proceeds in the following way. First of all one studies the operator

$$A_o = \begin{bmatrix} 0 & I \\ -A & -G_o \end{bmatrix} \ ,$$

where

$$(G_o v)(x) = -2\frac{\partial}{\partial x}\left[\ H(x)v'(x) \ \right] \ , \ H(x) = \int_0^L h(x,\xi) \ d\xi \ ,$$

the domain of A_o being defined in terms of a suitably adjusted set of boundary functionals, B_o. The boundary conditions corresponding to the subset $C \subset B$ remain unchanged as a subset of B_o, so the state space $\mathcal{H}$ remains unchanged. The problem of finding and estimating the normalized eigenfunction pairs (Φ_k, Ψ_k) and associated eigenvalues, Λ_k, for A_o is a complicated, but entirely standard [K], eigenvalue problem for a system of ordinary differential equations with boundary conditions of standard type. It can be seen, and the details will appear elsewhere, that the Λ_k asymptotically lie along the rays

$$\arg(z) = \pm\,(\pi/2 + \varepsilon)$$

in the left half complex plane, where ε, satisfying $0 < \varepsilon \leq \pi/2$, depends upon $\rho(x)$, $H(x)$ and $EI(x)$ only, not upon the boundary conditions specified via B_o. The eigenfunction pairs (Φ_k, Ψ_k) may be shown to form a Riesz basis for $\mathcal{H}$. It is possible that some finite number of the Λ_k have positive real part because $\mathcal{A}_o$ is not dissipative in general. The Riesz basis property of the (Φ_k, Ψ_k) together with the asymptotic location of the Λ_k are all that are required to show that $\mathcal{A}_o$ generates a holomorphic semigroup on $\mathcal{H}$ (cf. [F]).

Now let (φ_k, ψ_k) and λ_k denote the normalized eigenfunction pairs and associated eigenvalues for $\mathcal{A}$. It turns out that one can prove that

$$\lim_{|\lambda_k| \to \infty} (|\Lambda_k - \lambda_k|) = 0,$$

$$\sum_k \| (\Phi_k, \Psi_k) - (\varphi_k, \psi_k) \|^2 < \infty .$$

From the last relation, using a standard Hilbert space result (see [H], p. 208 ff.) it can be seen that the (φ_k, ψ_k) also form a Riesz basis for $\mathcal{H}$ so that $\mathcal{A}$ is seen also to generate a holomorphic semigroup on $\mathcal{H}$.

6. Spline / Finite Element Approximation.

According to the principle of virtual work [I], given $w(t)$, the trajectory of a mechanical system subject to holonomic constraints $H(w(t)) = 0$, with forces $f_i(t)$, $i = 1,2,\ldots,r$, acting on the system, the work done by these forces in a small virtual displacement from $w(t)$, at any instant t, vanishes. More precisely, if v is a vector such that

$$\frac{\partial H}{\partial w}(w(t))\ v = 0$$

then

$$\sum_{i=1}^{r} f_i(t)^* v = 0. \tag{6.1}$$

It should be noted that the sum (6.1) must include all forces acting on the system: inertial, restoring, damping, exogenous, etc. If a damping force, linearly dependent on velocity,

$$g(t) = - G\dot{w}(t),$$

where G is a non-negative self-adjoint operator (matrix in the finite dimensional case) is introduced into an otherwise conservative system whose kinetic energy is $\frac{1}{2}\dot{w}(t)^*M\dot{w}(t)$ and potential energy is $\frac{1}{2}w(t)^*Vw(t)$, M and V also non-negative self-adjoint, M positive definite, (6.1) may be expressed as

$$\left[-M\ddot{w}(t) - G\dot{w}(t) - Vw(t)\right]^* v = 0 \tag{6.2}$$

where $-M\ddot{w}$ is the inertial force, $-G\dot{w}$ is the damping force, and $-Vw$ is the restoring force for the system. Replacing v by $\dot{w}$ (which must be an admissible value for v) we obtain

$$\frac{d\mathcal{E}}{dt}\,(w(t),\dot{w}(t)) = -\dot{w}(t)^{*}G\dot{w}(t) \tag{6.3}$$

where $\mathcal{E}$ is the energy

$$\mathcal{E}(w(t),\dot{w}(t)) = \tfrac{1}{2}\left[\dot{w}(t)^{*}M\dot{w}(t) + w(t)^{*}Vw(t)\right] . \tag{6.4}$$

Formally, the derivation of the equation of motion,

$$M\ddot{w}(t) + G\dot{w}(t) + Vw(t) = 0, \tag{6.5}$$

is carried out via (6.2); in practice it is usually inferred from (6.3) after a quadratic form $-\dot{w}(t)^{*}G\dot{w}(t)$ expressing the energy loss through damping is hypothesized. In spatially distributed systems the forms in which G, V appear in (6.2) may be different from the forms in which they appear in (6.3), (6.5) due to transformation via integration by parts (use of the divergence theorem), appearance of boundary terms, etc.. For example, (6.3) might be expressed as a quadratic form in $\frac{\partial^2 w}{\partial x \partial t}$, but application of (6.2) requires that v should be an admissible velocity - not a partial derivative of such a velocity, necessitating a transformation by integration of parts.

To implement a spline, or general finite element, approximation procedure for the damped beam equation we begin with a finite dimensional vector Φ of coordinate functions

$$\Phi = \begin{bmatrix} \varphi_1 \\ \vdots \\ \varphi_n \end{bmatrix} . \tag{6.6}$$

We may, optionally, assume that

$$\langle \beta, \varphi_i \rangle = 0, \quad i = 1,2,\ldots,n, \quad (\beta,0) \in C,$$

so that the φ_i satisfy the kinematic constraints from the outset, or these constraints may be imposed in a later step to be described. For beam applications the basis functions φ_i, $i = 1,2,\ldots,n$, must be such that, with

$$w(x,t) = \sum_{i=1}^{n} w_i(t)\varphi_i(x) = \Phi * w(t) \ , \tag{6.7}$$

$$\frac{\partial w}{\partial t}(\xi,t) = \sum_{i=1}^{n} \dot{w}_i(t)\varphi_i(\xi) = \Phi(\xi) * \dot{w}(t) \ , \tag{6.8}$$

$$\frac{\partial^2 w}{\partial t \partial x}(\xi,t) = \sum_{i=1}^{n} \dot{w}_i(t)\varphi_i'(\xi) = \Phi'(\xi) * \dot{w}(t) \ , \tag{6.9}$$

are well-defined quantities at points ξ where external lateral forces and torques are to be applied.

Use of the representation (6.7), with concomitant expression of $\frac{\partial w}{\partial t}$, etc., as in (6.8), (6.9) implies movement of the beam is subject to certain holonomic constraints; infinitely many of them, in principle, the net effect of which is to allow the system to move in the finite dimensional subspace spanned by the coordinate functions φ_i, $i = 1,2,\ldots,n$. With such representation of $w(x,t)$, the work - energy relation with external lateral force σ and torque τ applied at the point $x = \xi$ may be seen to be

$$\frac{d}{dt}\left[\dot{w}(t) * Mw(t) + w(t) * Vw(t)\right] - \dot{w}(t) * G\dot{w}(t) = \sigma\Phi(\xi) * \dot{w}(t) + \tau\Phi'(\xi) * \dot{w}(t). \tag{6.10}$$

The functions φ_i are often chosen to be independent basis functions but this is not always convenient at the outset. If the φ_i are not independent there will be a set of r independent linear equations satisfied by the accompanying coefficients, which we may represent in the form

$$P\, w(t) = 0, \tag{6.11}$$

where P is an r x n matrix, $r \leq n - m < n$. Let the m x n matrix Q be such that $\begin{bmatrix} P \\ Q \end{bmatrix}$ is nonsingular and define $Q\, w = z$. We then have

$$\begin{bmatrix} P \\ Q \end{bmatrix} w(t) = \begin{bmatrix} 0 \\ z(t) \end{bmatrix} .$$

Writing $\begin{pmatrix} P \\ Q \end{pmatrix}^{-1} = (T,U)$, we find that $w(t) = U\, z(t)$ and, with

$$\tilde{M} \equiv U^*MU,\ \tilde{V} \equiv U^*VU,\ \tilde{G} \equiv U^*GU\ ,$$

we have, in place of (6.10),

$$\frac{d}{dt}\left[\dot{z}(t)^*\tilde{M}\dot{z}(t) + z(t)^*\tilde{V}z(t)\right] - \dot{z}(t)^*\tilde{G}\dot{z}(t)$$

$$= \sigma(t)\ \Phi(\xi)^*U\dot{z}(t) + \tau(t)\ \Phi'(\xi)^*U\dot{z}(t)\ , \qquad (6.12)$$

leading to the equations

$$\tilde{M}\,\ddot{z}(t) + \tilde{G}\,\dot{z}(t) + \tilde{V}\,z(t) = \sigma(t)\ U^*\Phi(\xi) + \tau(t)\ U^*\Phi'(\xi) \qquad (6.13)$$

as the equations of motion for the system.

The kinematic boundary conditions, corresponding to C as described above, may be imposed via (6.11) if desired. The other boundary conditions, corresponding to B - C, are never imposed explicitly; they come about as particular cases of the dynamical equations in (6.13).

If the coordinates to be retained are a subset of the components of w, we can write $w^* = (\tilde{w}^*, \hat{w}^*)$, where $\tilde{w}$ comprises the components to be discarded and $\hat{w}$ the components to be retained. Then P is partitioned accordingly: $P = (\tilde{P}, \hat{P})$, and we can assume that the r x r matrix $\tilde{P}$ is nonsingular. Then, with $m = n - r$,

$$\tilde{w} = -(\tilde{P})^{-1}\hat{P}\,\hat{w}\ ,\ w = \begin{pmatrix} -(\tilde{P})^{-1}\hat{P} \\ I_m \end{pmatrix} \hat{w} \equiv U\,\hat{w}$$

and we obtain (6.13) again, replacing z(t) by $\hat{w}(t)$. Computationally this is easier because $\tilde{P}$ is r x r while $\begin{pmatrix} P \\ Q \end{pmatrix}$ is n x n.

In actual computational work it is preferable to define the energy and dissipation forms in the continuous context and then approximate them by quadratic forms on finite dimensional spaces.

Application of (6.11), (6.12) to the approximate energy and dissipation forms then leads to the finite dimensional approximating equations of motion in the form (6.13) with symmetric matrices $\tilde{M}$, $\tilde{G}$, and $\tilde{V}$. This procedure is much easier and more reliable than first deriving the equations of motion as partial differential equations in the continuous case and then proceeding to solve those equations numerically, taking into account all of the boundary conditions. In fact, by the recommended procedure, only the kinematic boundary conditions are actually enforced explicitly. The example of the next section should be helpful in clarifying these matters.

7. Approximation and Simulation for the Cantilever Beam System.

Let the interval $\ell = [0,L]$ be divided into m subintervals

$$I_k = \left[(k-1)\frac{L}{m},\ k\frac{L}{m}\right] = [x_{k-1},x_k] = [x_{k-1},x_{k-1}+h],\ h = L/m,\ k = 1,2,\ldots$$

and consider general quadratic functions on the intervals I_k:

$$q_k(x) = a_k + b_k(x-x_{k-1}) + c_k(x-x_{k-1})^2 .$$

The functions defined on I_k by 1, $x-x_{k-1}$, $(x-x_{k-1})^2$, and extended by 0 to the rest of ℓ correspond to the functions φ_i, $i = 1,2,\ldots,n$, $n = 3m$, discussed in the previous section. With

$$a(t)^* = (a_1(t),\ldots,a_m(t)),\ b(t)^* = (b_1,\ldots,b_m(t)),$$

$$c(t)^* = (c_1(t),\ldots,c_m(t)),$$

$$\Phi^*(x) = \left[\chi_{I_1},\ldots,\chi_{I_m},x\cdot\chi_{I_1},\ldots,(x-x_{m-1})\cdot\chi_{I_m},x^2\cdot\chi_{I_1},\ldots,(x-x_{m-1})^2\cdot\chi_{I_m}\right],$$

and $w(t)^* = (a(t)^*,b(t)^*,c(t)^*)$, we can define a function $w(x,t)$, piecewise quadratic in x, with possible discontinuities at the points x_k, $k = 1,2,\ldots,m-1$, by

$$w(x,t) = \Phi(x)^* w(t).$$

We proceed to define the energy and dissipation forms in terms of these functions, ignoring the discontinuities for the present.

Assuming the beam to have mass density ρ, the kinetic energy is

$$\mathcal{T} = \frac{\rho}{2}\int_0^L \left\{\frac{\partial w}{\partial t}(x,t)\right\}^2 dx = \frac{\rho}{2}\sum_{k=1}^{m}\int_{x_{k-1}}^{x_k}\left[\dot{a}_k(t)+\dot{b}_k(t)(x-x_{k-1})+\dot{c}_k(t)(x-x_{k-1})^2\right]dx =$$

$$\frac{\rho}{2}\left\{ h\dot{a}_k(t)^2+\frac{h^3}{3}\dot{b}_k(t)^2+\frac{h^5}{5}\dot{c}_k(t)+h^2\dot{a}_k(t)\dot{b}_k(t)+\frac{2}{3}h^3\dot{a}_k(t)\dot{c}_k(t)+\frac{1}{2}h^4\dot{b}_k(t)\dot{c}_k(t)\right\}$$

$$= \frac{\rho}{2}\,\dot{w}(t)^{*}M\dot{w}(t)\ ,$$

from which we see that

$$M = \begin{pmatrix} hI_m & \frac{1}{2}h^2I_m & \frac{1}{3}h^3I_m \\ \frac{1}{2}h^2I_m & \frac{1}{3}h^3I_m & \frac{1}{4}h^4I_m \\ \frac{1}{3}h^3I_m & \frac{1}{4}h^4I_m & \frac{1}{5}h^5I_m \end{pmatrix} .$$

Here I_M denotes the m x m identity matrix.

Next we pass to the potential energy which, for constant bending modulus EI, is

$$\frac{1}{2}EI\sum_{k=1}^{m}\int_{x_{k-1}}^{x_k}\left(\frac{\partial^2 w}{\partial x^2}(x,t)\right)^2 dx = \frac{1}{2}EI\sum_{k=1}^{m}\int_{x_{k-1}}^{x_k}4\dot{c}_k(t)^2 dx$$

$$= 2EIh\dot{c}_k(t)^2$$

so that

$$V = \begin{pmatrix} 0 & 0 & 0 \\ 0 & 0 & 0 \\ 0 & 0 & 4EIhI_m \end{pmatrix} .$$

Passing now to the dissipation form, we first of all take the interraction kernel $h(x,\xi)$ to have the form $\gamma h(x-\xi)$ where, assuming that m will always be a multiple of a fixed positive integer μ,

$$h(\eta) = 1,\ |\eta| \leq L/\mu\ ,\ h(\eta) = 0 \text{ otherwise.}$$

We define $\nu = \nu(m) = m/\mu$ for all values of m used. For the case $m = 9$, $\nu = \mu = 3$, the support of $h(x-\xi)$ is the shaded region shown in Figure 7.1.

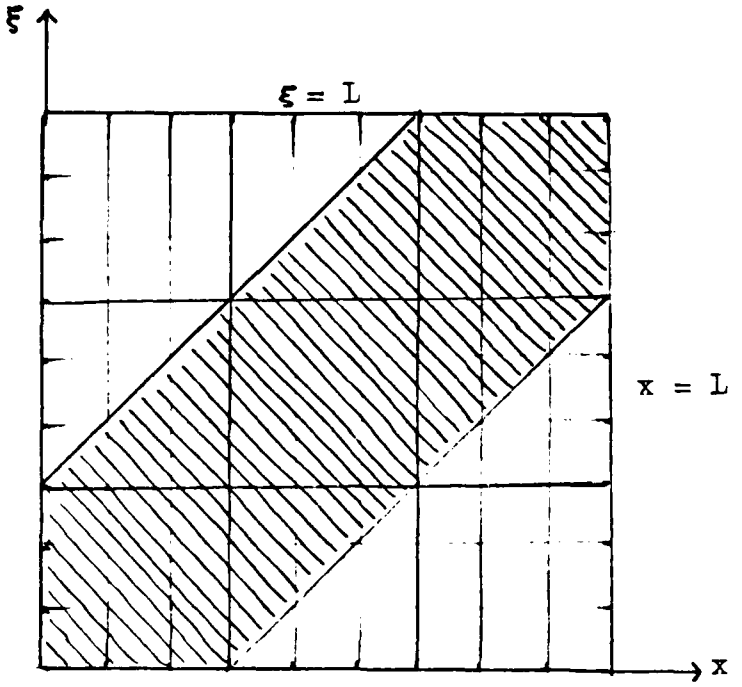

Fig. 7.1

Let

$$S_k^\ell = \left\{ (x,\xi) \;\middle|\; x_{k-1} \leqq x \leqq x_k \;,\; x_{\ell-1} \leqq \xi \leqq x_\ell \right\} .$$

Then in S_k^ℓ we have

$$\frac{\partial^2 w}{\partial t \partial x}(x,t) - \frac{\partial^2 w}{\partial t \partial x}(\xi,t) = \dot{b}_k(t) + 2\dot{c}_k(t)(x-x_{k-1}) - \dot{b}_\ell(t) - 2\dot{c}_\ell(t)(\xi-\xi_{\ell-1})$$

For $|k-\ell| < \nu$ we square this quantity and integrate over S_k^ℓ; then sum over the indicated values of k,ℓ to obtain the quadratic form

$$\dot{w}(t)^* G_\nu w(t) = 2\gamma \sum_{k,\ell} (\dot{a}(t)^*, \dot{b}(t)^*, \dot{c}(t)^*) \begin{bmatrix} 0 & 0 & 0 \\ 0 & h^2 J_{k,\ell} & h^3 J_{k,\ell} \\ 0 & h^3 J_{k,\ell} & h^4 K_{k,\ell} \end{bmatrix} \begin{bmatrix} \dot{a}(t) \\ \dot{b}(t) \\ \dot{c}(t) \end{bmatrix}$$

where

$$\left[J_{k,\ell}\right]_k^k = 1, \quad \left[J_{k,\ell}\right]_\ell^\ell = 1, \quad \left[J_{k,\ell}\right]_\ell^k = -1, \quad \left[J_{k,\ell}\right]_k^\ell = -1 ,$$

$$\left[J_{k,\ell}\right]_j^i = 0 \text{ otherwise;}$$

$$\left[K_{k,\ell}\right]_k^k = \tfrac{4}{3},\ \left[K_{k,\ell}\right]_\ell^\ell = \tfrac{4}{3},\ \left[K_{k,\ell}\right]_\ell^k = -1,\ \left[K_{k,\ell}\right]_k^\ell = -1\ ,$$

$$\left[K_{k,\ell}\right]_j^i = 0 \text{ otherwise}\ .$$

Additionally we must treat the upper and lower borders of the region of support of $h(x-\xi)$, consisting of triangles $\tilde{T}_k$, $\hat{T}_k$, $k = 1,2,\ldots,M-\nu$ as shown in Figure 7.1. After integration of the same function as shown earlier over these regions, followed by summation over the relevant indices, we obtain

$$\dot{w}(t)^* G_1 \dot{w}(t) = 2\gamma \sum_{k=1}^{m-\nu} (\dot{a}(t)^*, \dot{b}(t)^*, \dot{c}(t)^*) \begin{bmatrix} 0 & 0 & 0 \\ 0 & h^2 J_{k,\ell} & h^3 K_{k,\ell} \\ 0 & h^3 K_{k,\ell} & h^4 L_{k,\ell} \end{bmatrix} \begin{bmatrix} \dot{a}(t) \\ \dot{b}(t) \\ \dot{c}(t) \end{bmatrix}$$

with $J_{k,\ell}$ and $K_{k,\ell}$ as above and

$$\left[L_{k,\ell}\right]_k^k = 2,\ \left[L_{k,\ell}\right]_\ell^\ell = 2,\ \left[L_{k,\ell}\right]_\ell^k = -1,\ \left[L_{k,\ell}\right]_k^\ell = -1\ ,$$

$$\left[L_{k,\ell}\right]_j^i = 0 \text{ otherwise;}$$

After G_0 and G_1 have been computed as indicated we set $G = G_0 + G_1$.

Next there is the matter of the construction of the reduction matrix U. From the representation on I_k

$$w(x,t) = a_k(t) + b_k(t)(x-x_{k-1}) + c_k(t)(x-x_{k-1})^2\ ,$$

$$\frac{\partial w}{\partial x}(x,t) = b_k(t) + 2c_k(t)(x-x_{k-1})\ ,$$

we see that $w(x,t)$ is piecewise C^2 on $\mathcal{L}$ just in case, for $k = 1,2,\ldots,m-1$ we have

$$a_{k+1}(t) = a_k(t) + b_k(t)h + c_k(t)h^2 ,$$

$$b_{k+1}(t) = b_k(t) + 2c_k(t)h .$$

For the cantilever case of our example we have, in addition,

$$a_1(t) = 0, \; b_1(t) = 0 .$$

Accordingly, we have the following linear relationships holding between the coefficients

$$\left[\begin{array}{cccccccccccccccc}
1 & 0 & 0 & \cdots & 0 & 0 & 0 & 0 & 0 & \cdots & 0 & 0 & 0 & 0 & \cdots & 0 & 0 \\
-1 & 1 & 0 & \cdots & 0 & 0 & 0 & -h & 0 & \cdots & 0 & 0 & -h^2 & 0 & \cdots & 0 & 0 \\
0 & -1 & 1 & \cdots & 0 & 0 & 0 & -h & 0 & \cdots & 0 & 0 & 0 & -h^2 & \cdots & 0 & 0 \\
\vdots & \vdots & \vdots & & \vdots & \vdots & \vdots & \vdots & \vdots & & \vdots & \vdots & \vdots & \vdots & \vdots & \vdots & \vdots \\
0 & 0 & 0 & & -1 & 1 & 0 & 0 & 0 & \cdots & -h & 0 & 0 & 0 & \cdots & -h^2 & 0 \\
0 & 0 & 0 & \cdots & 0 & 0 & 1 & 0 & 0 & \cdots & 0 & 0 & 0 & 0 & \cdots & 0 & 0 \\
0 & 0 & 0 & \cdots & 0 & 0 & -1 & 1 & 0 & \cdots & 0 & 0 & -2h & 0 & \cdots & 0 & 0 \\
0 & 0 & 0 & \cdots & 0 & 0 & 0 & -1 & 1 & \cdots & 0 & 0 & 0 & -2h & \cdots & 0 & 0 \\
\vdots & \vdots & \vdots & & \vdots & \vdots & \vdots & \vdots & \vdots & & \vdots & \vdots & \vdots & \vdots & \vdots & \vdots & \vdots \\
0 & 0 & 0 & & 0 & 0 & 0 & 0 & 0 & \cdots & -1 & 1 & 0 & 0 & \cdots & -2h & 0
\end{array}\right]
\left[\begin{array}{c} a_1 \\ \vdots \\ a_m \\ b_1 \\ \vdots \\ b_m \\ c_1 \\ \vdots \\ c_m \end{array}\right] = 0 .$$

$$\underbrace{\qquad\qquad\qquad\qquad}_{\tilde{P}} \qquad \underbrace{\qquad\qquad\qquad\qquad}_{\hat{P}}$$

Let R be the matrix with

$$R^i_j = -1, \; j = i + 1, \quad r^i_j = 0 \text{ otherwise.}$$

Then, with $Q = I + R$ we have

$$\tilde{P} = \left[\begin{array}{cc} I + R & hR \\ 0 & I + R \end{array}\right] = \left[\begin{array}{cc} Q & hR \\ 0 & Q \end{array}\right]$$

is readily inverted, giving

$$\begin{Bmatrix} \tilde{P} \end{Bmatrix}^{-1} = \begin{bmatrix} Q^{-1} & -h(Q^{-1} - Q^{-2}) \\ 0 & Q^{-1} \end{bmatrix} .$$

Since

$$\hat{P} = \begin{Bmatrix} h^2 R \\ 2hR \end{Bmatrix} = \begin{Bmatrix} h^2(Q-I_m) \\ 2h(Q-I_m) \end{Bmatrix}$$

we obtain, as the reduction matrix

$$U = \begin{Bmatrix} -\tilde{P}^{-1}\hat{P} \\ I_m \end{Bmatrix} = \begin{bmatrix} h^2 I_m - 3h^2 Q^{-1} + 2h^2 Q^{-2} \\ 2h(Q^{-1} - I_m) \\ I_m \end{bmatrix} .$$

Then a further easy computation shows that

$$Q^{-1} = \begin{bmatrix} 1 & 0 & 0 & \dots & 0 \\ 1 & 1 & 0 & \dots & 0 \\ 1 & 1 & 1 & \dots & 0 \\ \vdots & \vdots & \vdots & & \vdots \\ 1 & 1 & 1 & \dots & 1 \end{bmatrix} , \quad Q^{-2} = \begin{bmatrix} 1 & 0 & 0 & \dots & 0 \\ 2 & 1 & 0 & \dots & 0 \\ 3 & 2 & 1 & \dots & 0 \\ \vdots & \vdots & \vdots & & \vdots \\ m & m-1 & m-2 & \dots & 1 \end{bmatrix} .$$

We see therefore that the reduction matrix U can be computed explicitly without having to resort to numerical matrix inversion in this example. Once this has been done the matrices $\tilde{M}$, $\tilde{G}$ and $\tilde{V}$ of (6.12) can be calculated readily and, using a Cholesky decomposition to write $\tilde{M}$ in the form $\mathfrak{L}\mathfrak{L}^*$, with $\mathfrak{L}$ lower triangular, the equation (6.13) can be pre- and post-multipled by $\mathfrak{L}^{-1}$ and $(\mathfrak{L}^*)^{-1}$, respectively, to yield an equation for which the corresponding first order system matrix is

$$\mathcal{A} = \begin{bmatrix} 0 & I_m \\ -\mathfrak{L}^{-1}\tilde{V}(\mathfrak{L}^*)^{-1} & -\mathfrak{L}^{-1}\tilde{G}(\mathfrak{L}^*)^{-1} \end{bmatrix} .$$

We have calculated this matrix, and subsequently its eigenvalues, for a cantilever beam with $\rho = 1$, $\gamma = .01$, $EI = 100$ and length $L = 10$. The interaction kernel $h(x-\xi)$ was taken to be constant with support restricted to $|x-\xi| \leq L/2$. In Figures 7.2(a) and (b)

we show the eigenvalue patterns in the upper left half plane for m = 14, 16 and 24 (not all of the eigenvalues are shown in the last case). Figure 7.2(b) magnifies the lower right hand corner of Figure 7.2(a) in order to show the pattern of the eigenvalues corresponding to low frequencies more clearly. Variational considerations account for the decrease in the natural frequencies as M gets larger but the increasing negative real parts of eigenvalues, or exponential damping rates, came as somewhat of a surprize. This property, if it can be substantiated in general, would be quite desirable for applications because it would mean that damping rates are systematically underestimated in approximations of this sort, providing a safety factor in control applications. From Figure 7.2 it is seen that the quadratic dependence of the damping rate on frequency at the low end of the spectrum has only the most limited range.

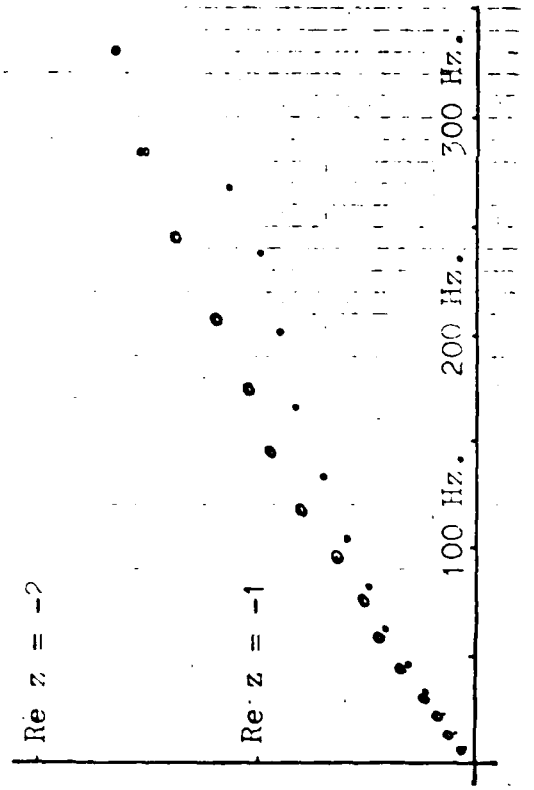

Fig. 7.2(a)

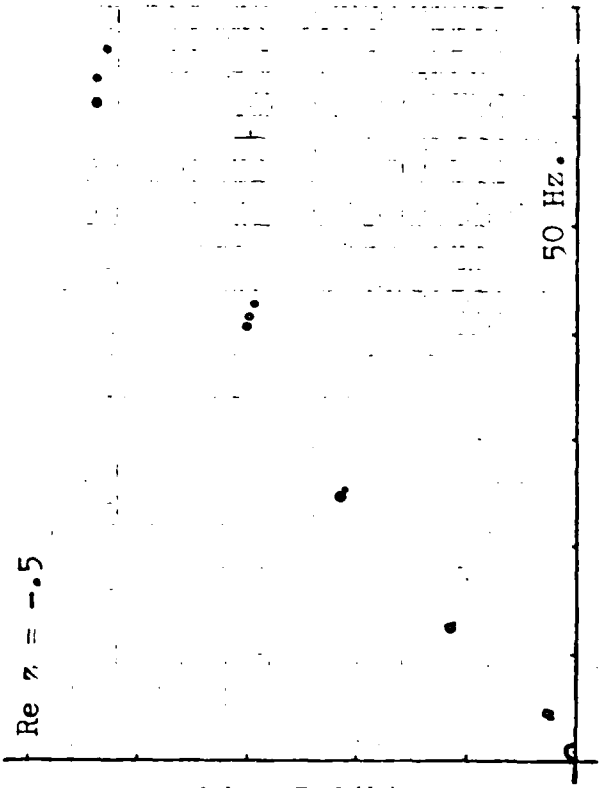

Fig. 7.2(b)

(Small dots indicate the location of eigenvalues for M = 14. Hollow dots correspond to M = 16 and large solid dots show eigenvalues corresponding to M = 24. Where the last two are too close to be separated on the graph, a hollow dot with a heavy outer boundary is shown.)

8. Some Theory Related to Laboratory Experimentation.

The foregoing results from mathematical simulation can be, and have been, compared with related data taken from elastic beam experiments in a laboratory setting. This, of course, is nothing new by itself but perhaps we can claim that we are in a position to look at such data in a different light than most of our predecessors. The author is fortunate to have access to extensive electronic equipment for collecting and analyzing data in the UW MIPAC (Modelling, Information Processing and Control) Facility and great advantage has been taken of this experimental capability during the last two years. Before describing the results of this experimentation program and the relationship of these results to the mathematical simulation discussed above, we digress briefly to describe the experimental context and some of the inherent problems attendant upon the observation of vibrating beams in the laboratory.

The laboratory beam configurations easiest to realize, at least approximately, are those involving either clamped ends or free ends. The results which we cite in Section 9 were obtained in the clamped / free (cantilever) setting and in a "pseudo" free / free configuration. The clamped / clamped beam is easy enough to work with, and we have conducted some experiments in this context, but we do not report on this case here, mainly because we have only one clamp really adequate to the task. That the task of realizing a good approximation to a clamped beam endpoint is not at all trivial will be commented on at some length later in this section. The free / free case is qualified by the word "pseudo" because, in fact, the beam is actually suspended vertically by a very fine nylon thread. The two experimental configurations are illustrated in Figure 8.1(a),(b).

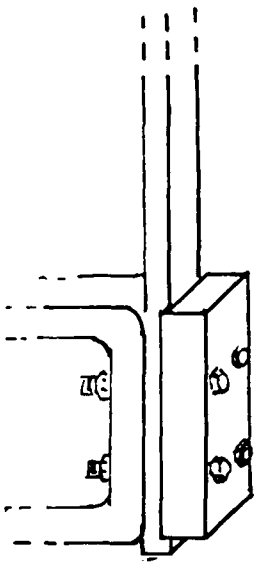

Fig. 8.1(a)

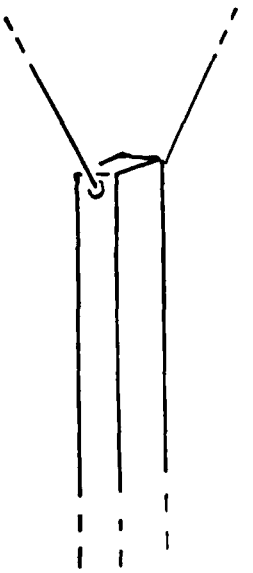

Fig. 8.1(b)

Let us begin by discussing this pseudo free / free case; from now on we simply refer to it as the pseudo free configuration. To obtain a reasonable facsimile of the free beam, whose actual realization requires a gravity-free environment achievable only in space or free fall conditions with accompanying difficulties as regards excitation and measurement, we suspend an elastic beam from a suitable support, preferably a high one, by a long, very fine, nylon filament; for our purposes 3 lb. test nylon fishing line served admirably. The accelerometer is attached to the beam at the lower - truly free - end. Just attaching the accelerometer introduces a variety of problems in itself but we avoid that difficulty in the present article.

We proceed now to discuss the coupled beam / filament system in some detail. We will do this as if the beam were supported by a single filament although a double filament arrangement such as is shown in Fig. 8.1(b) is used in practice.

We are interested in energy losses from the beam through the supporting filament, so we will model the beam itself via the energy

conservative Euler-Bernoulli equation. Assuming the beam to have length L, uniform linear mass density ρ and bending modulus EI, all constant, and assuming the cord supporting the beam to have length ℓ and linear mass density r, we have as the approximate energy expression for the system

$$\frac{1}{2}\int_0^L \left[\rho \left(\frac{\partial w}{\partial t}\right)^2 + EI \left(\frac{\partial^2 w}{\partial x^2}\right)^2 \right] dx + \frac{1}{2} g\rho L \left[\frac{v(0,t)}{\ell}\right]^2$$

$$+ \frac{1}{2}\int_0^{\ell} \left[r \left(\frac{\partial v}{\partial t}\right)^2 + \rho L \left(\frac{\partial v}{\partial s}\right)^2 \right] ds ,$$

with the constraint $w(L,t) = v(0,t)$. Here w is the beam deflection as a function of x and v is the string deflection as a function of s. From this energy form one readily derives the equations

$$\rho \frac{\partial^2 w}{\partial t^2} + EI \frac{\partial^4 w}{\partial x^4} = 0, \quad 0 \leq x \leq L , \tag{8.1}$$

$$r \frac{\partial^2 w}{\partial t^2} - \rho L \frac{\partial^2 w}{\partial s^2} = 0, \quad 0 \leq s \leq \ell , \tag{8.2}$$

and the boundary conditons

$$\frac{\partial^2 w}{\partial x^2}(0,t) = 0, \quad \frac{\partial^3 w}{\partial x^3}(0,t) = 0, \quad \frac{\partial^2 w}{\partial x^2}(L,t) = 0 , \tag{8.3}$$

$$EI\frac{\partial^3 w}{\partial x^3}(L,t) + \rho L \frac{\partial v}{\partial s}(0,t) + \frac{g\rho L}{\ell} w(L,t) = 0 . \tag{8.4}$$

At $s = \ell$ we assume no reflection:

$$\frac{\partial v}{\partial t}(\ell,t) + \left(\frac{\rho L}{r}\right)^{1/2} \frac{\partial v}{\partial s}(\ell,t) = 0 . \tag{8.5}$$

It is not supposed that the last condition is completely realistic. It simply replaces more complicated assumptions ensuring that very little, if any, energy entering the the supporting filament, or string, is reflected back to the beam. We are assuming that waves

in the string move only in the direction from s = 0 to s = ℓ. Then, in fact, equation (8.5) is valid with ℓ replaced by s, $0 \leq s \leq \ell$; in particular it is true at s = 0. Using this in (8.4) along with the constraint w(L,t) = v(0,t) we arrive at

$$EI \frac{\partial^3 w}{\partial x^3}(L,t) + \left[\frac{g\rho L}{\ell} - (r\rho L)^{1/2} \right] \frac{\partial w}{\partial t}(L,t) = 0 . \qquad (8.6)$$

Since we assume ℓ large and r small,

$$\tau \equiv (r\rho L)^{1/2} - \frac{g\rho L}{\ell}$$

is a small positive number and the boundary condition (8.6) becomes

$$EI \frac{\partial^3 w}{\partial x^3}(L,t) - \tau \frac{\partial w}{\partial t}(L,t) = 0 . \qquad (8.7)$$

If we define

$$a = (\rho/EI)^{1/4}$$

and assume solutions of the form

$$w(x,t) = e^{i\omega^2 t} w(x)$$

with ω complex, the resulting eigenfunction equation is

$$w^{(iv)} - (a\omega)^4 w = 0 . \qquad (8.8)$$

Applying the boundary conditions (8.3) and (8.7) to the general solution of (8.8), and setting

$$\lambda = a\omega , \quad \sigma = \tau/a^2 ,$$

we obtain the determinantal condition

$$\det \begin{bmatrix} -\cos \lambda L + \cosh \lambda L & \sin \lambda L + \sinh \lambda L \\ \lambda \sin \lambda L + \lambda \sinh \lambda L & -\lambda \cos \lambda L + \lambda \cosh \lambda L \\ -\sigma i \cos \lambda L - \sigma i \cosh \lambda L & -\sigma i \sin \lambda L - \sigma i \sinh \lambda L \end{bmatrix} = 0 ,$$

which simplifies to

$$2\lambda - 2\lambda \cos \lambda L \cosh \lambda L + 2\sigma i \cos \lambda L \sinh \lambda L - 2\sigma i \sin \lambda L \cosh \lambda L = 0.$$

If we let

$$\lambda = \left[\frac{2k - 1}{2} \right] \frac{\pi}{L} + \varepsilon\lambda$$

and substitute into this equation, we find that, to first order in $\varepsilon\lambda$ we have

$$\varepsilon\lambda\left[\cosh\left(\frac{2k-1}{2}\right)\pi - \frac{2\sigma i L}{2(k-1)\pi}\sinh\left(\frac{(2k-1)\pi}{2}\right)\right] \simeq (-1)^k + \frac{2\sigma i}{(2k-1)\pi}\cosh\left(\frac{(2k-1)\pi}{2}\right),$$

and from this it is easy to see that, to first order in $1/k$,

$$\varepsilon\lambda \simeq \frac{2\sigma i}{(2k-1)\pi} .$$

Then, to zero order in $1/k$,

$$i\omega^2 = i\,\frac{\lambda^2}{a^2} = i\,\frac{(2k-1)^2\pi^2}{4a^2L^2} - \frac{2\sigma}{a^2L} .$$

Asymptotically, then, the damping of the k-th mode of the beam due to the presence of the supporting filament is uniform and the damping exponent

$$\frac{2\sigma}{a^2L} = \frac{2EIr}{\rho L} = \frac{2EI}{\rho L}\left[(r\rho L)^{1/2} - \frac{g\rho L}{\ell}\right]$$

tends to zero as $r \to 0$ and $\ell \to \infty$, i.e., as the supporting cord becomes very light and very long. We judge, therefore, that this type of support mechanism will not lead to damping rates comparable at high frequencies to those arising from internal sources in our laboratory experiments.

A somewhat similar analysis shows that losses due to excitation of acoustic waves in the surrounding atmosphere by the high frequency vibrations of the beam will also be asymptotically uniform and thus

not likely to be confused with internal damping effects.

It has been recognized by various experimenters for some time that clamped beam experiments are subject to substantial degrees of interference from the interraction between the beam and the nearly, but not quite, rigid clamping device. In order to have some means for evaluating the likely degree of error in damping experiments under these circumstances, we ask the reader to consider with us a clamping arrangement in which the beam to be tested is, as shown in Fig. 8.2, the relatively thin beam lying in the region $x > 0$, except for a portion embedded in the more massive beam which occupies the region $x < 0$ and which serves in our "thought experiment" (our apologies to the memory of the originator of that useful expression!) as the clamping device, stiff but not entirely rigid - the unintended result of most of our laboratory clamping attempts.

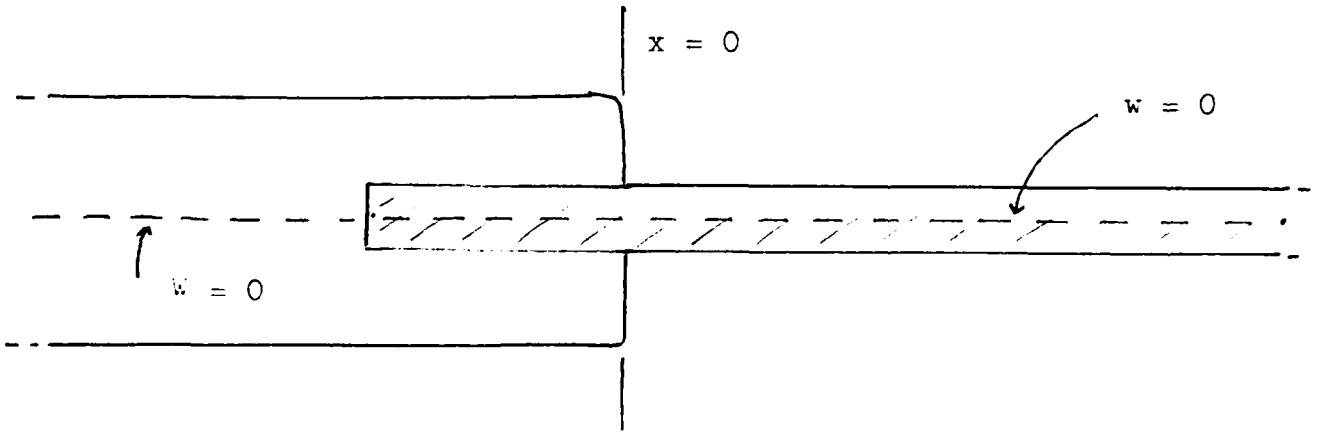

Fig. 8.2

We denote lateral displacement of the thin beam by $w(x,t)$, $x \geq 0$, and lateral displacements of the thick beam by $W(x,t)$, $x \leq 0$. We will study "monochromatic", i.e., single frequency, solutions of the combined system under the assumption that "outgoing" waves, moving toward $-\infty$, in the clamping beam are eventually absorbed and not reflected back to $x = 0$.

Adopting complex notation, we represent the displacement of the

thin beam by

$$w(x,t) = \beta e^{i(\omega^2 t - \alpha\omega x)} + \gamma e^{i(\omega^2 t + \alpha\omega x)}, \qquad (8.9)$$

where $\alpha^4 = (\rho/\varepsilon\iota)$, ρ and $\varepsilon\iota$ being the linear mass density and bending modulus, respectively, of the thin beam. The first term represents waves moving outward from $x = 0$ to ∞ while the second term represents waves moving inward toward $x = 0$ from ∞. Because of our assumption that all waves in the thick beam originate at $x = 0$ and are not reflected back subsequently, we represent the thick beam displacement by

$$W(x,t) = \delta e^{i(\omega^2 t + A\omega x)}, \qquad (8.10)$$

where $A^4 = (R/EI)$, R, EI the linear mass density and bending modulus, respectively, of the heavy beam. It is easy to see that the condition that no work should be done on the combined system at $x = 0$ is

$$EI \frac{\partial^2 W}{\partial x^2}(0,t) - \varepsilon\iota \frac{\partial^2 w}{\partial x^2}(0,t) = 0,$$

$$EI \frac{\partial^3 W}{\partial x^3}(0,t) - \varepsilon\iota \frac{\partial^3 w}{\partial x^3}(0,t) = 0,$$

where EI and $\varepsilon\iota$ have been defined above. Applied to (8.9) and (8.10) these yield

$$\begin{bmatrix} \varepsilon\iota\alpha^2\omega^2 & \varepsilon\iota\alpha^2\omega^2 & -EIA^2\omega^2 \\ i\varepsilon\iota\alpha^3\omega^3 & -i\varepsilon\iota\alpha^3\omega^3 & EIA^3\omega^3 \end{bmatrix} \begin{bmatrix} \beta \\ \gamma \\ \delta \end{bmatrix} = \begin{bmatrix} 0 \\ 0 \end{bmatrix}.$$

Normalizing γ to 1 we find that

$$\delta = \frac{2\varepsilon\iota\alpha^3}{EIA^2(A+\alpha)}, \quad \beta = \frac{A - \alpha}{A + \alpha}.$$

It is convenient to renormalize β to $A - \alpha$, γ to $A + \alpha$ so that

$$w(x,t) = (A - \alpha)e^{i(\omega^2 t - \alpha\omega x)} + (A + \alpha)e^{i(\omega^2 t + \alpha\omega x)}. \qquad (8.11)$$

If the two beams are of the same material, so that $E = \varepsilon$, then, since ι becomes small more rapidly than ρ as the thickness of the thin beam decreases, we shall have $0 < A < \alpha$, $-1 < \beta < 0$ so that the outgoing, i.e., reflected, wave in the thin beam has uniformly smaller modulus than the incoming wave, independent of the frequency / wavelength.

Computing the boundary values of $\frac{\partial w}{\partial t}$, $\frac{\partial^2 w}{\partial x^2}$, $\frac{\partial^2 w}{\partial t \partial x}$ and $\frac{\partial^3 w}{\partial x^3}$ at $x = 0$ with the formula (8.11) for $w(x,t)$, we arrive at dissipative frequency dependent boundary conditions

$$\frac{\partial^2 w}{\partial x^2}(0,t) = \frac{\alpha}{\omega} \frac{1}{(A+\alpha)^2-(A-\alpha)^2} \frac{\partial^2 w}{\partial t \partial x}(0,t) = \frac{1}{4A\omega} \frac{\partial^2 w}{\partial t \partial x}(0,t),$$

$$\frac{\partial^3 w}{\partial x^3}(0,t) = -\alpha^3 \omega \frac{1}{(A+\alpha)^2-(A-\alpha)^2} \frac{\partial w}{\partial t}(0,t) = \frac{-\alpha^2 \omega}{4A} \frac{\partial w}{\partial t}(0,t).$$

It may be computed that the energy associated with the travelling wave of wave length $2\pi/\alpha\omega$, call it $\mathcal{E}(\omega,t)$, computed over a suitable finite, moving domain with 0 as its left hand boundary in order to avoid $\mathcal{E}$ being infinite, decays according to

$$\frac{d\mathcal{E}(\omega,t)}{dt} = -8A\rho\omega^5$$

while the energy itself, over a large domain as described, may be seen to be proportional to ω^4. We conclude, as a result, that the energy decay rate exponent must be directly proportional to the square root of the frequency, ω^2, under these circumstances. It is clear that such a damping relationship may seriously interfere with accurate measurement of the internal exponential damping rate, even though we expect the latter to be proportional to ω^2 rather than ω. While actual clamping mechanisms are not really thick beams as supposed here, this analysis is, we feel, sufficiently realistic to at least partially explain the very severe difficulties encountered in trying to measure the damping rates of the natural modes of clamped beams in the laboratory.

9. Some Experimental Results.

In a laboratory experiment the beam is excited by striking it smartly in order to set it into vibration. A record such as the one shown in Figure 9.1 is obtained; in this case the record exhibited is the graph of an input voltage to UW MIPAC's HP5451C System Analyzer proportional to the free endpoint lateral velocity of a cantilever beam clamped at the other end.

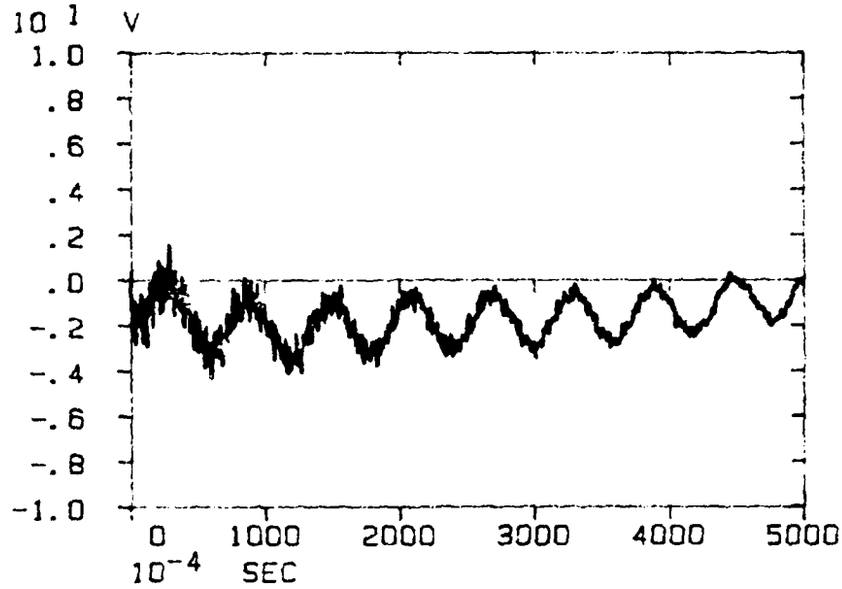

Fig. 9.1

The record initially shows a substantial high frequency component, as evidenced by the jagged character of the graph on the left hand side. As the motion continues we observe that the curve becomes smoother, evidence that the high frequency component is becoming smaller in relation to the overall amplitude of the motion. In fact, the amplitude of the fundamental mode is not very different at the end of the time interval from what it was at the beginning; very little damping is observed at this low frequency.

To obtain a better appreciation of the quantitative factors involved in the evolution of the beam's motion, the record is divided into a number of successive segments of equal length. The (Fast) Fourier transform of each segment is computed and multiplied by its conjugate to yield the power spectrum for that interval. For most

purposes it is desirable to form the logarithm of the power spectrum, which we henceforth call the logarithmic power spectrum. This is what is displayed in Figure 9.2 (though for a different input record than the one shown in Figure 9.1). Here two successive logarithmic power spectra are superimposed to yield the complete diagram. The peaks evident in each graph correspond to the frequencies of the natural modes of vibration. Since it is the logarithm which is displayed, the vertical gaps between peaks of successive spectra are proportional to the (negative) real part of the complex system eigenvalue associated with that mode of vibration while the horizontal position of the peak corresponds to the imaginary part of the eigenvalue, i.e., to the frequency of that mode.

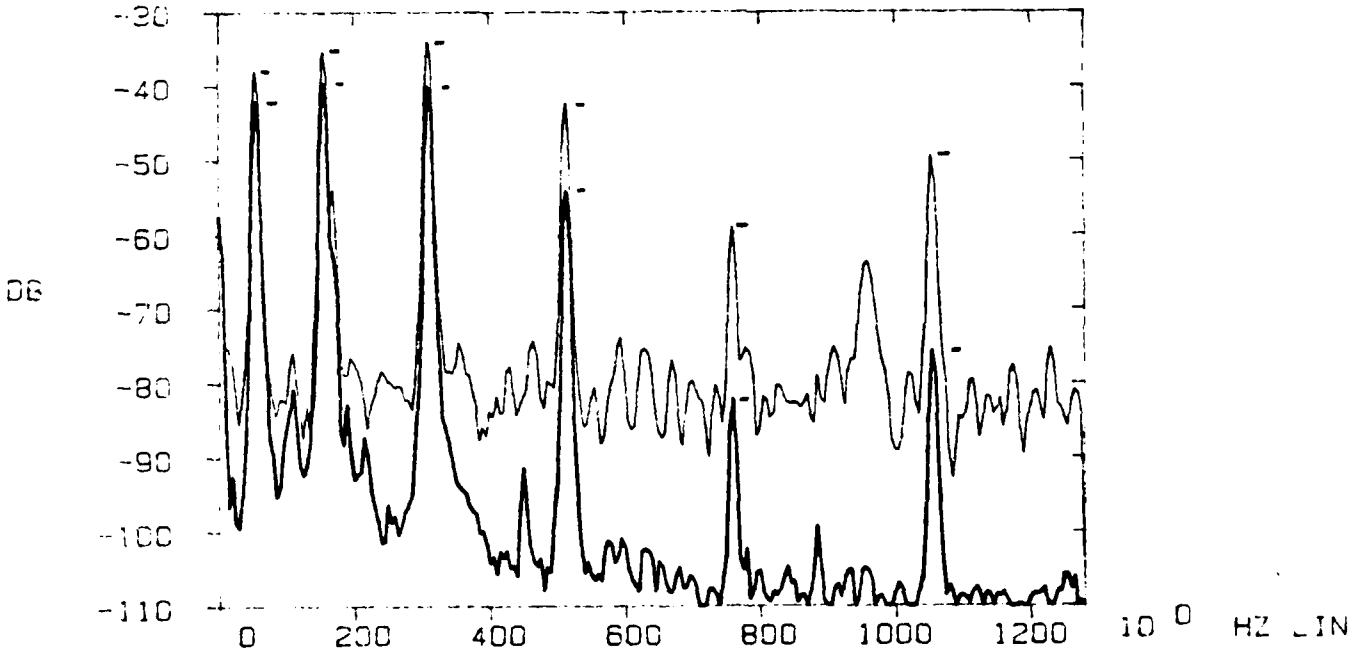

Fig. 9.2

Figures 9.2 through 9.4 display logarithmic power spectra from a "pseudo-free" boron-epoxy composite beam, a clamped wooden beam, and a "pseudo - free" metallic beam , respectively. In these figures we have added short horizontal bars to more clearly indicate the successive peak positions. The data is averaged over many experiments, using the same beam, recording data over an interval of the same length, but exciting the beam in different ways in order to adequately sample all modes. The approximately linear relationship between damping ratio and frequency is strikingly evident for the wooden and composite beams, less so, but still fairly convincing, for the metallic beam.

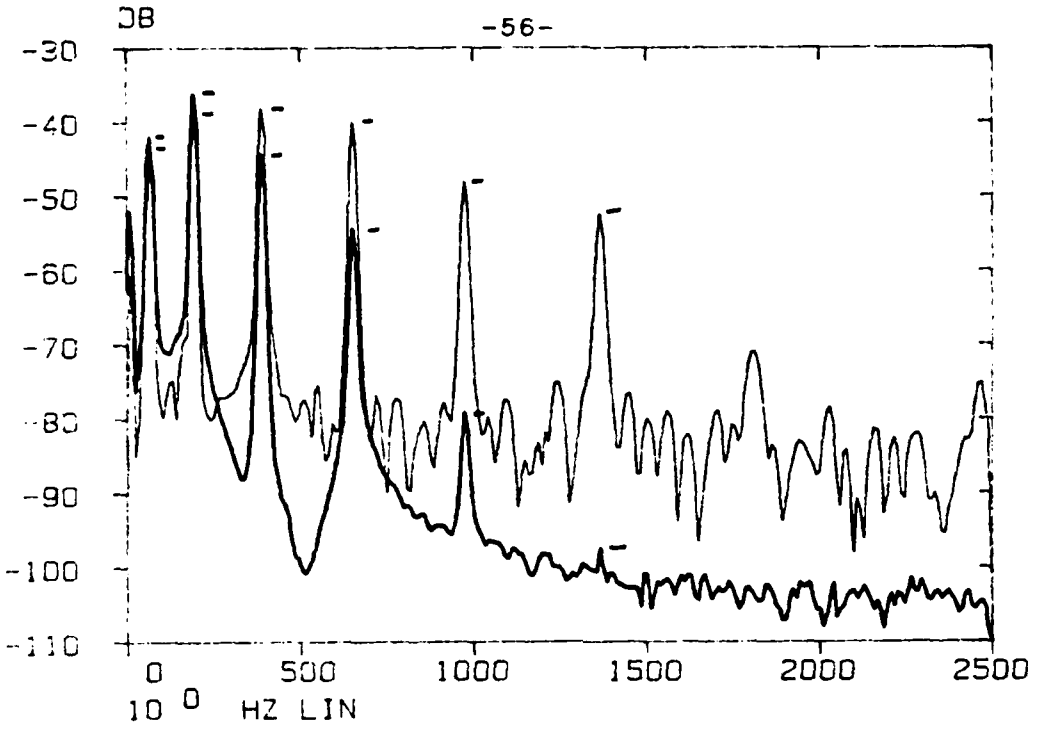

Fig. 9.3

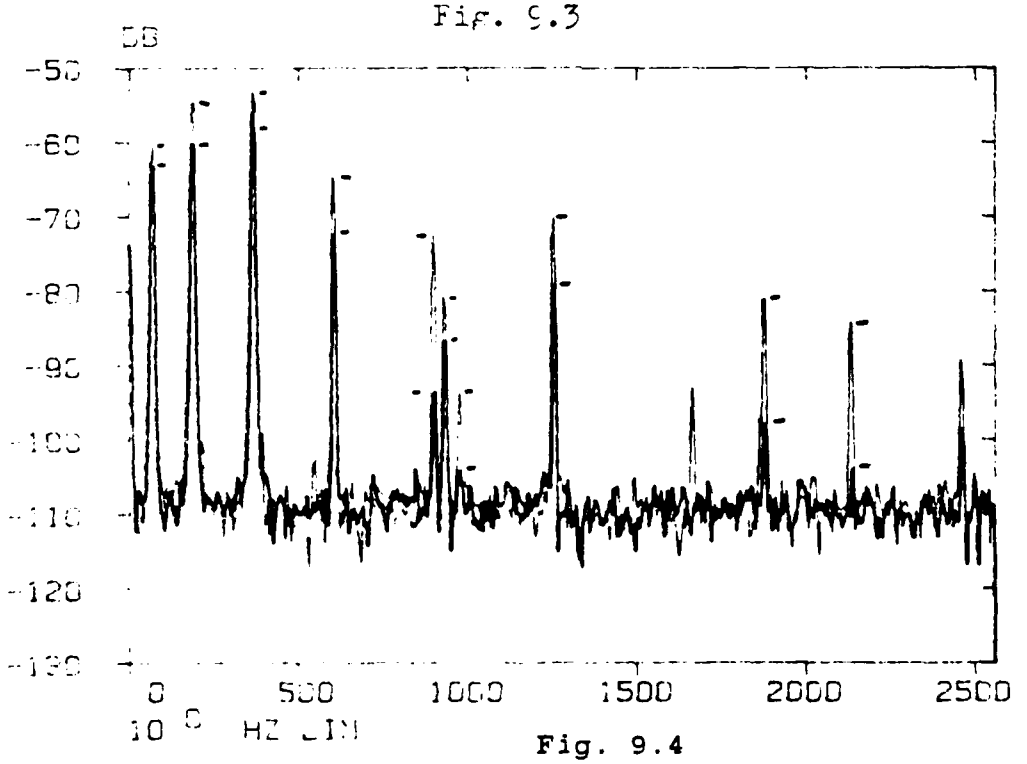

Fig. 9.4

It might be natural as a result of this evidence of frequency proportional damping in elastic beams to suppose that all comparable elastic structures exhibit the same sort of relationship between damping and frequency. Indeed, this was the author's initial predisposition. It is here that continued experimentation in the laboratory

teaches us not to trust our instincts too implicitly. Figure 9.5 shows successive logarithmic power spectra obtained from longitudinal vibrations of a steel rod, approximately one meter long and 1.5 cm. in diameter in its circular cross section. The accelerometer is mounted on one end and the other end is struck sharply with a heavy steel hammer. Through the first three modes the damping rates grow quite rapidly but then settle down to nearly constant rates, exhibiting no demonstrable dependence on frequency from 10 khz. through 50 khz. . This experiment has been repeated many times with much the same results in all cases.

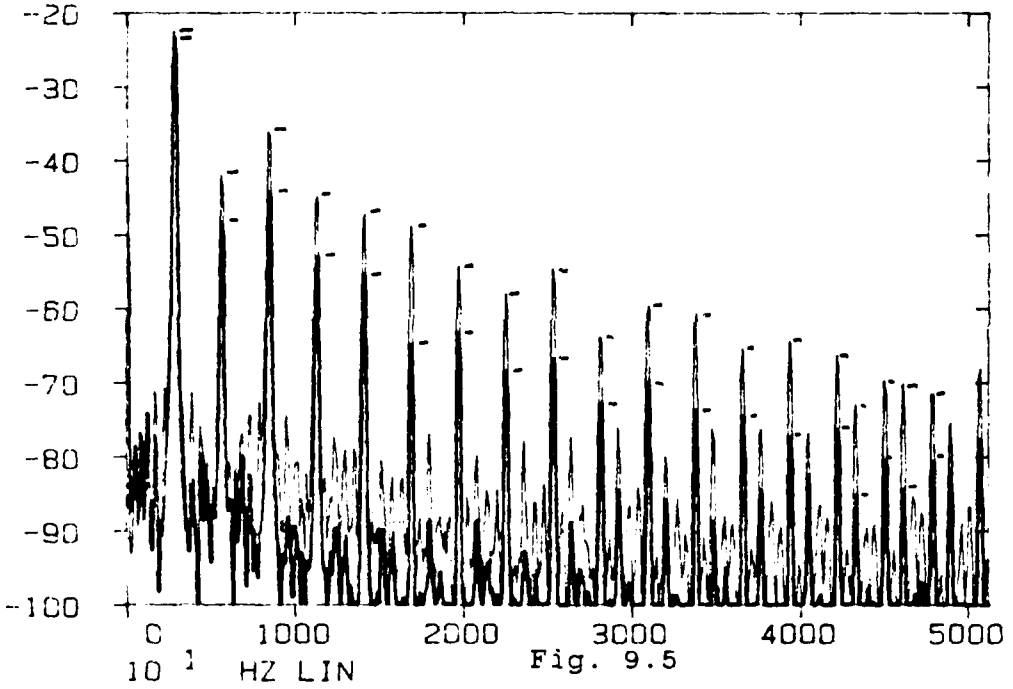

Fig. 9.5

In reality, this result is quite consistent with frequency proportional damping in the Euler ~ Bernoulli beam and with our earlier suppositions as to the source of the damping action. If the same assumptions are made in regard to the internal structure of the rod as were made for the beam, the resulting model for vibrations in the rod takes the form of the damped wave equation (constant coefficient case only shown here)

$$r\frac{\partial^2 z}{\partial t^2} + 2\gamma \int_0^L \ell(x-\xi)\left[\frac{\partial z}{\partial t}(x,t) - \frac{\partial z}{\partial t}(\xi,t) \right] d\xi - E\,\frac{\partial^2 z}{\partial x^2} = 0, \quad (9.1)$$

$z(x,t)$ denoting the longitudinal displacement of the rod element

whose equilibrium center of mass is at x and $\ell(\eta)$ an interraction kernel of the same sort as $h(\eta)$ used earlier for the beam. Analysis similar to that used for the infinite beam in Section 4 shows that a damping spectrum of the type observed in Fig. 9.5, i.e., quadratic damping exponent versus frequency dependence for small ω and asymptotically constant as $\omega \to \infty$, results for the infinite rod and, correspondingly, similar discrete behavior is to be expected for a finite rod. So we may tentatively accept (9.1) as a viable model for longitudinal, internally damped vibrations of a rod.

With (9.1) so accepted, we now envision an idealized beam constructed, as shown in Figure 9.6, from two such rods rigidly spaced a distance 2δ apart, with a mass-less, perfectly flexible, but inextensible central support structure forming the "back - bone" of the system. Lateral displacements of the structure will be described in terms of the graph of the locus of the center line, $w = w(x,t)$, as shown in the figure.

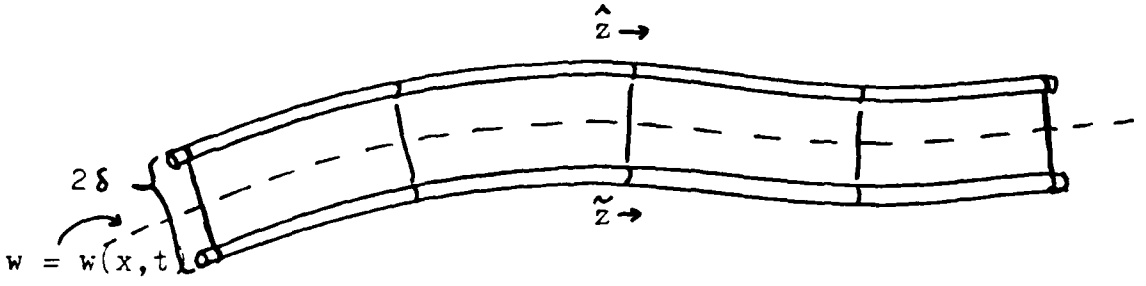

Fig. 9.6

Using the energy expression

$$E(z,\frac{\partial z}{\partial t}) = \frac{1}{2}\int_0^L \left[r\left(\frac{\partial z}{\partial t}\right)^2 + E\left(\frac{\partial z}{\partial x}\right)^2 \right] dx$$

for longitudinal rod vibrations, we find with use of (9.1) and the appropriate boundary conditions, e.g.,

$$\frac{\partial z}{\partial x}(0,t) = \frac{\partial z}{\partial x}(L,t) = 0 \tag{9.2}$$

in the case of free ends, that for smooth solutions we have

$$\frac{dE}{dt}(z,\frac{\partial z}{\partial t}) = -\gamma \int_0^L\int_0^L \ell(x-\xi)\Big[\frac{\partial z}{\partial t}(x,t) - \frac{\partial z}{\partial t}(\xi,t)\Big]^2 d\xi dx. \tag{9.3}$$

Let $\hat{z}(x,t)$, $\tilde{z}(x,t)$ denote the longitudinal displacements of the upper and lower rods of the beam structure, respectively. Then we find, to first order in δ, that

$$\frac{\partial \hat{z}}{\partial x}(x,t) = -\delta \frac{\partial^2 w}{\partial x^2}(x,t), \quad \frac{\partial \tilde{z}}{\partial x}(x,t) = \delta \frac{\partial^2 w}{\partial x^2}(x,t) .$$

Letting

$$\mathcal{E}(w,\frac{\partial w}{\partial t}) = E(\hat{z},\frac{\partial \hat{z}}{\partial t}) + E(\tilde{z},\frac{\partial \tilde{z}}{\partial t}) + \int_0^L r\Big[\frac{\partial w}{\partial t}\Big]^2 dx \tag{9.4}$$

we have, with $\rho = 2r$, $I_\rho = \rho\delta$, $EI = 2\delta^2 E$,

$$\mathcal{E}(w,\frac{\partial w}{\partial t}) = \frac{1}{2}\int_0^L \Big[\rho\Big[\frac{\partial w}{\partial t}\Big]^2 + I_\rho\Big[-\frac{\partial^2 w}{\partial t \partial x}\Big]^2 + EI\Big[\frac{\partial^2 w}{\partial x^2}\Big]^2\Big] dx \tag{9.5}$$

while the dissipation form (9.3) becomes, with

$$h(x-\xi) = 2\delta^2 \ell(x-\xi),$$

$$\frac{d\mathcal{E}}{dt}(w,\frac{\partial w}{\partial t}) = -\gamma \int_0^L\int_0^L h(x-\xi)\Big[-\frac{\partial^2 w}{\partial t \partial x}(x,t) - -\frac{\partial^2 w}{\partial t \partial x}(\xi,t)\Big]^2 d\xi dx. \tag{9.6}$$

Assuming $I_\rho = \rho\delta$ is very small in comparison with both ρ and EI (i.e., we assume δ very small and E very large), the condition that

the time derivative of (9.5) with respect to t should be (9.6) leads to the equation (3.7), with $h(x,\xi) = \gamma h(x-\xi)$ there, and the associated boundary conditions. If I_ρ is not neglected we obtain the corresponding Rayleigh model with damping term as in the Euler-Bernoulli model (3.7). Thus the rod model (9.1) is consistent with our earlier developed beam models. Significantly, as we remarked at the end of Section 4, for the damped Rayleigh model the high frequency damping exponent predicted by that model has the same properties as has been observed in the laboratory (Figure 9.5) and as are predicted from the model equation (9.1).

10. Concluding Remarks.

In this paper we have attempted to:

(i) Show that laboratory beams of various types do exhibit modes whose damping exponents are proportional to frequency at the high end of the spectrum;

(ii) Show that there is a relatively simple mathematical model which exhibits comparable spectral behavior and whose form is explainable in terms of plausible physical properties of the beam;

(iii) Show that numerical calculations using a spline based approximation of our mathematical model yield calculated spectral values qualitatively consistent with those obtained from laboratory experimentation and predicted from analysis of the mathematical model.

Some readers may object that the motivation of the damping term in our equation (3.7) is based on a heuristic, plausibility argument rather than on the accepted *modus operandi* of introducing an appropriate constitutive equation and deriving the dynamics from that point of departure.[8] About all we can say in defense of ourselves on this point is that we are probably not the best person equipped to do this; we have presented sufficient motivation to allow others who specialize in continuum mechanics to carry out such a program if they are inclined to do so. Along the same lines, we also realize that our interpretation of the action of the damping term in terms of fiber structure of the beam, or comparable action of extended crystal structures, may well turn out to be inadequate in the light of other information about the manner in which damping forces act in elastic structures.

We do, without apology, insist that laboratory measurement of damping rates, though necessarily flawed to some extent by exogenous influences, which we have taken some pains to analyze here, must be the final arbiter in deciding between putative damping mechanisms. Even spotlessly correct theoretical reasoning cannot ultimately take precedence - though it could indicate the need for more careful laboratory work. Hundreds of experiments on our part do indicate

frequency proportional damping at the high end of the spectrum and some sort of quadratic behavior, or at least the dominance of a different proportionality constant, at lower frequencies. We invite other interested researchers to carry out similar experimentation and model development complementing, or perhaps even replacing, that reported here.

The reality of near quadratic dependence of the damping exponent on frequency at the low end of the spectrum seems to us to be a very important question. Just citing the models introduced in this article, whether or not this phenomenon is real appears to be the decisive factor in choosing the model which we have proposed in preference to "square root" damping as in (2.3) which we have, for the present at least, rejected as not adequately explainable in physical terms - though we have conceded that it could be justified in terms of distances covered by travelling waves of a given frequency. If it could be conclusively demonstrated that low frequency modes are damped at rates which bear the same relationship to frequency as the damping rates associated with higher frequency modes then the whole modelling process would have to be reconsidered in that light. To settle this matter it would seem to be necessary to conduct experiments with very long beams having a large number of low frequency modes.

It also seems to us that the frequency independent damping of higher modes apparently applying to longitudinal rod vibrations is a critical test of the theory. It is particularly significant that this mode of damping is consistent with the very different sort of damping observed in the beam and it is intriguing that the mode of damping which apparently applies for the rod is what is necessary to preserve controllability by means of finite dimensional controls. If frequency proportional damping exponents did apply to longitudinal vibrations of the rod, those vibrations would be uncontrollable in either the sense standard for the one dimensional wave equation [L] or that which applies to parabolic processes [M]. The whole area is a most intriguing one. If this article should serve to encourage more researchers to enter the area, even if only to refute our contributions, this article will have served its purpose.

REFERENCES

[A] Antman, S. S., and T.-P. Liu: "Travelling waves in hyperelastic rods", Quart. Appl. Math., January 1979.

[B] ---, and R. Malek-Madani: "Dissipative mechanisms", Proc. of the IMS, Minneapolis. To appear.

[C] Fung, Y. C.: "Foundations of Solid Mechanics", Prentice-Hall, Englewood Cliffs, NJ, 1965

[D] Love, A. E. H., "A Treatise on the Mathematical Theory of Elasticity", 4th ed., Cambridge University Press, 1927

[E] Chen, G., and D. L. Russell: "A mathematical model for linear elastic systems with structural damping", Quart. Appl. Math., January 1982.

[F] Kato, T.: "Perturbation Theory for Linear Operators", Springer-Verlag, New York, 1966.

[G] Phillips, R. S.: "Dissipative operators and hyperbolic systems of partial differential equations", Trans. Am. Math. Soc. 90 (1959) pp. 123 - 254.

[H] Riesz, F., and B. Sz. Nagy: "Functional Analysis", F. Ungar Pub. Co., New York, 1955.

[I] Goldstein, H.: "Classical Mechanics", Addison - Wesley Pub. Co., Inc., Reading, Mass., 1950.

[J] Timoshenko, S. P.: "Vibration Problems in Engineering", 2nd Ed., D. Van Nostrand & Co., Inc., Princeton, NJ, 1955

[K] Coddington, E. A., and N. Levinson: "Theory of Ordinary Differential Equations", McGraw-Hill Book Co., New York, 1955

[L] Russell, D. L.: "Controllability and stabilizability theory for linear partial differential equations", SIAM Rev. 20 (1978), pp. 639 - 739.

[M] Fattorini, H. O., and D. L. Russell: "Exact controllability theorems for linear parabolic equations in one space dimension", Arch. Rat. Mech. & Anal. 43(1971), pp. 272 - 292.

[N] Bert, C. W.: "Material damping: an introductory review of mathematical models, measures and experimental techniques", Journal of Sound and Vibration 29 (1973), pp. 129 - 153.

[O] ---, and R. R. Clary: "Evaluation of experimental methods for determing dynamic stiffness and damping of composite materials", Special Technical Publication 546, American Society for Testing and Materials, Philadelphia, 1974.

[P] Lazan, B. J.: "Damping of Materials and Members in Structural Mechanics", Pergamon Press, Oxford, 1968.

[Q] Kimball, A. L., and D. E. Lovell: "Internal friction in solids", Physical Review Series 2, 30 (1927), pp. 948 - 959.

[R] Bishop, R. E. D.: "The treatment of damping forces in vibration theory", Journal of the Royal Aeronautical Society, 59 (1955), pp. 738 - 742.

[S] Hurty, W. C., and M. F. Rubinstein: "Dynamics of Structures", Prentice - Hall, Inc., Englewood Cliffs, NJ, 1964.

1 OCT 1991

Approved for public release IAW AFR 190-12.
Distribution is unlimited.
MATTHEW J. KELLY
Chief, Technical Information Division

END

1-87

DTIC